Specific Heat Capacity of Pure Water at 4.0 MPa between 298.15 K and 465.65 K

Joan J. Manyà[a,b], Michael Jerry Antal, Jr.[c], Christopher K. Kinoshita[c], and Stephen M. Masutani[c]

Hawaii Natural Energy Institute, School of Ocean and Earth Science and Technology, University of Hawaii at Manoa, Honolulu, Hawaii 96822 and Thermo-chemical Processes Group (GPT), Aragón Institute of Engineering Research (I3A), University of Zaragoza, Maria de Luna 3, E-50018 Zaragoza, Spain.

[a] To whom correspondence should be addressed.

E-mail address: joanjoma@unizar.es Fax: + 34 976761879

[b] Aragón Institute of Engineering Research (I3A), University of Zaragoza

[c] University of Hawaii at Manoa

Abstract

The present work reports experimental results concerning the specific isobaric heat capacity of pure water at elevated pressure. Experiments were performed using a Tian-Calvet differential scanning calorimeter (Setaram model BT2.15), at temperatures ranging from 298.15 K to 465.65 K and at a constant pressure of 4.0 MPa. The aim of this study is to compare the new experimental results with values predicted by the IAPWS-95 formulation, which is generally accepted as reliable by the scientific community despite the fact that, in this formulation, nearly all the data for the isobaric heat capacity of water are based on measurements of Sirota's group in the former Soviet Union in the period from 1956 to 1970. The present calorimetric results for the specific heat capacity of pure water were found to be substantially in disagreement with the values obtained using the IAPWS-95 formulation, especially at high temperatures, where the differences are greater than 20%. Additional studies are therefore warranted in order to confirm this discrepancy.

Keywords

Heat Capacity; Tian-Calvet Calorimeter; Pure Water; IAPWS-95

Introduction

Of all pure engineering fluids, water is among the most important substances in existence.[1] It is used as a working fluid in steam power cycles which supply electricity in large amounts to the industrialized world and for numerous other technical applications. In addition to its use in the energy sector, water is the most widely used solvent in chemical and biological systems.

It is well-known that thermodynamic properties of aqueous electrolyte solutions at elevated temperatures are important in understanding various electrochemical and geochemical processes, such as the performance of alkaline biocarbon fuel cells[2, 3] and the study of CO_2 storage in saline aquifers.[4, 5] Models for determining properties of aqueous electrolyte solutions that work over wide ranges of composition, temperature, and pressure are thus in demand and the development of such models continues to be an important subject of research. To achieve this aim, it is absolutely necessary (among other things) to secure accurate data on the standard-state partial molar heat capacities of the electrolytes being modeled.

In 1995, the International Association for the Properties of Water and Steam (IAPWS) adopted a new formulation called ‘‘The IAPWS Formulation 1995 for the Thermodynamic Properties of Ordinary Water Substance for General and Scientific Use.’’ In that work, which was described by Wagner and Pruss[1], nearly all the data for the isobaric heat capacity (C_p) for water are based on measurements of Sirota’s group in the former Soviet Union in the period from 1956 to 1970.[1, 6] Since then, only two further C_p data sets have been published that were used for fitting the IAPWS-95 formulation. These are the measurements of Angell et al.[7], who investigated subcooled liquid water at ambient pressure, and the high-pressure C_p data (up to 1.0 GPa at a constant temperature of 299.65 K) measured by Czarnota[8] in 1984. Wagner and Pruss[1] reported that the IAPWS-95 formulation, which is in the form of a fundamental equation explicit in the Helmholtz free energy, showed slightly better agreement with the mentioned C_p experimental data[1] than the previous IAPS-84 formulation (which is based on the fundamental equation developed by Haar, Gallagher and Kerr[9]). More recently, Archer and Carter[10] published C_p measurements for subcooled liquid water, which cover almost the same region as the data of Angell and coworkers.[7] In any case, it seems reasonable to verify the experimental reliability of calorimetric data obtained many years ago, especially for high-temperature and high-pressure measurements in the liquid phase (i.e., for conditions where calorimetric measurements can be affected by large systematic errors).

The instrument of measurement used by Sirota and coworkers[6] was a flow calorimeter developed at the F. E. Dzerzhinskii All-Union Institute of Thermal Technology, and constructed in the 1950s.[11] The method of continuous-flow calorimetry is based on the fact that the material being investigated is sequentially pumped through two flow calorimeters: a "main" calorimeter (which operates at the desired pressure and temperature conditions) and a reference one (which works at the same pressure but at room temperature). Similar calorimetric devices were used in Europe and in North America. In fact, the development in 1971 of an innovative mass-flow calorimeter (also called as Picker-type flow calorimeter) by Desnoyers and coworkers[12] facilitated the direct measurement of the heat capacity of aqueous solutions. The main advantage of using flow calorimeters is the elimination of the vapor space. However, heat transfer from the calorimetric tubing (and the heater) to the surroundings has been generally recognized as a principal source of systematic errors during the measurement by means of a flow calorimeter.[13–15] Attempts to correct for these heat losses (which increase strongly with temperature due to radiation[16]) were generally based on the adoption of a particular aqueous solution as a chemical standard.[15] Desnoyers and coworkers[17] recommended NaCl(aq) as the chemical standard for calibration. The drawback of this procedure is that the reference values were determined from measurements previously made by similar calorimeter devices.

It is important to note that no new relevant data on the specific heat capacity of pure water at different pressures have been reported in the recent years, in spite of the large number of published works, which have been focused on measuring the apparent partial molar heat capacity of aqueous solutions (see, for instance, the works of Ballerat-Busserolles and coworkers[18], Jones and coworkers[19], Magalhaes and coworkers[20], Patterson and coworkers[21] and Schrödle and coworkers[22]). Among the few exceptions are the studies of Lourenço and coworkers[23] and Sampaio and Nieto de Castro[24], in which the heat capacity of water was measured as a supplemental check on the performance of the experimental setup (which employed a Setaram DSC-111 differential scanning calorimeter) for temperatures ranging from 299 K to 370 K (at 0.1 MPa). In that work, the obtained values were in reasonably good agreement with those generated from the Wagner and Pruss[1] equation of state for water (deviations lower than 1.5%).

As mentioned above, experimental measurements of C_p in liquids are subject to several problems largely derived from their volatility. Some calorimeters typically used to determine C_p in liquids (e.g., the Picker-type flow calorimeters[17, 25]) must operate at near room temperature and are thus, scarcely flexible as regards temperature adjustment. In addition, both Picker-type flow and twin-cell adiabatic calorimeters can only operate at a single temperature in each experiment;

hence, determining the temperature dependence of the heat capacity, C_p (T), is labor intensive and time-consuming.[26] Although differential scanning calorimetry (DSC) is not a standard technique for determining liquid heat capacities, it is the most suitable choice when measurements as a function of temperature are required.[26] In addition, the continuing development of the fixed DSC calorimeters has improved their precision, which is currently comparable to that of both Picker-type flow and twin-cell adiabatic calorimeters (see, for instance, the comparison reported by Woolley[25]).

The goal of the present work was to perform measurements of the specific isobaric heat capacity of pure water, using a Tian-Calvet differential scanning calorimeter, at temperatures ranging from 298.15 K to 465.65 K and at a pressure of 4.0 MPa. This pressure value corresponds to the normal working pressure of an alkaline biocarbon fuel cell[2] and is within the safe operating range of our instrument. In addition, this pressure value offers a good safety margin against boiling at the upper range of temperatures we investigated. The obtained values must be extensively analyzed in order to assess their reliability. In this sense, all possible systematic error sources should be taken into account during the experimental data validation.

Experimental Section

Differential Scanning Calorimeter

The instrument used in this study was a Tian-Calvet heat flow batch calorimeter from Setaram (model BT2.15), which has an operating temperature range of 77 K to 473 K. Sub-ambient temperature operation of the instrument is possible due to an integrated liquid nitrogen cooling loop. Figure 1 illustrates the major elements of the experimental system. The calorimeter operation is based on the Calvet's principle: the calorimetric signal is the differential heat flow rate, which is measured by one thermopile around each vessel.[26] More in detail, the calorimeter consists of two thermal fluxmeters, each constructed by a series of 480 thermocouples surrounding a cylindrical cavity. The fluxmeters are arranged symmetrically around the two cells (a reference cell and a sample cell) in an aluminum block located in the cavity. The signal delivered by the power difference of the two fluxmeters is proportional to the heat effects occurring in the cells. The temperature of the calorimeter block is monitored by means of a Pt-100 resistance thermometer located between the two cells. Only the temperature of the calorimeter block is recorded. It is not possible to measure the temperature of the sample in the cell directly. To accurately estimate the temperature inside the sample cell as a function of the

temperature of the calorimeter block, a calibration process was carried out by the manufacturer by use of a calibrated Pt-100 probe embedded in a stainless steel block of the same geometry as the calorimetric cells. This process was performed at different heating rates and the corrections were smoothed with a polynomial equation, the coefficients of which were implemented in the software of the instrument.

The reference cell was a Setaram Regular Batch Cell with a volume of 12 cm^3. This vessel was a cylindrical Hastelloy container with a cap, tightly closed without any link with the outside. For all of the experiments performed in this study, the reference cell was kept empty, except for air. The sample cell (a Setaram High Pressure Gas Circulation cell with a volume of 8.5 cm^3, see Figure 2 for details) was made in stainless steel 316 and can operate at pressures up to 10 MPa with a maximum temperature of 473 K. The sample cell was charged with research grade nitrogen to the desired pressure using the system displayed in Figure 1. The pressure inside the sample cell was kept constant by means of a large buffer volume (two stainless steel tanks with a total volume of 1.5 L). A pressure transducer (Cole-Palmer C-68971-23 with an accuracy of ±0.15% full scale) was used to measure the system pressure. During the course of a typical experiment, pressure changes were very small (of the order of ±0.17%).

Water Samples

The water used in the present study was sequentially deionized (resistivity ≥ 18 MΩ cm) and degassed. For the last purpose, a helium flow rate of approximately 1 dm^3 min^{-1} was sparged through 100 cm^3 of deionized water at room temperature during 20 min. After that, the helium-saturated water was filtered under vacuum in order to remove the helium present. The pure water samples were stored under nitrogen atmosphere in sealed glass containers to avoid the absorption of CO_2 from the air. All manipulations of the water samples were made under nitrogen atmosphere using an inert glove box.

Experimental Procedure

The experiments with pure water were performed at two different pressure values: 0.1 and 4.0 MPa. The experiments at atmospheric pressure provided useful information regarding the accuracy of both the measurement and data processing procedures that we employed, since the specific heat capacity of water at 0.1 MPa predicted by the IAPWS-95 formulation has been experimentally confirmed by several recent studies.[23, 27]

Two types of heating protocols were selected to conduct the calorimetric measurements: a continuous heating program and a stepwise heating method. The second method requires more time but it can be more accurate as it is less affected by long-term drifts of the baseline and by

systematic errors due to heat-transfer-related variations.[22, 28] Table 1 reports the details concerning both heating programs.

In all of the experiments, the amount of sample used was 2 cm^3 (at room temperature, m = 1.9986 ± 0.0193 g). The pressurized sample cell was partially filled with water and, consequently, the system allows the liquid sample volume to change freely during heating. However, a correction factor must be considered because the amount of inert gas present into the cell is lower than the case in which the sample cell is empty (blank test). In addition, the use of this type of cell (gas circulation cell) instead a constant-volume cell (which is only suitable for low pressures) implies an additional source of uncertainty: the experimental heat capacity includes a contribution from the enthalpy of vaporization. While the terms due to the enthalpy of vaporization are negligible at low vapor pressures, a correction is required as the boiling temperature of the solutions is approached. The correction factor is a function of the quantity of the sample in the cell, the vapor pressure of the components, and the (vapor + liquid) equilibrium distribution of the mixture components.[29]

Verification of Calorimeter Performance

Several tasks were performed in order to ensure the accuracy of the instrument: (a) measurement of the heat flow signal repeatability for blank tests (empty cells); (b) both temperature and heat flow measurements for indium at a pressure of 4.0 MPa; and (c) heat capacity measurements for synthetic sapphire at atmospheric pressure. All of these tasks are described below.

Blank tests repeatability

For each of four experimental conditions (pressure and heating program) summarized in Table 1, three measuring tests were carried out with the sample cell empty (blank test) in order to check the repeatability of the measured heat flow data. As an example, Figure 3 displays the data corresponding to the continuous heating program at 4.0 MPa. As can be seen from the figure, the similarity between the three replicates is excellent. The same behavior was observed for the rest of experimental conditions analyzed. The relative high signal values obtained for the blank tests could be due to the fact that the sample cell is different compared to the reference cell (from both geometrical and physical points of view). In addition, some difference can be explained by the fact that the sample cell is filled with nitrogen at 4.0 MPa (the reference cell is filled with atmospheric pressure air). In this sense, the thermal effects related to the relatively high amount of nitrogen present in the sample cell during the heating period can partially explain the measured heat flow signal.

To statistically analyze the variation due to the measuring device (or repeatability), a crossed gage R&R study (using the ANOVA method) was conducted using Minitab® 15 on the data generated in the three blank tests (under continuous heating program at 4.0 MPa). A crossed gage R&R study estimates how much total process variation is caused by the measurement system.[30] For this purpose, the heat flow signals corresponding to 18 temperatures (from 293.15 to 463.15 K in steps of 10 K) were considered as measured parts for the analysis. Figure 4a displays the output results of the gage R&R study. Only a small fraction of the total variation (1.12%) was due to the measurement system; therefore, the repeatability of the system is very good. In addition to this, Figure 4b shows the interval plot for the means at 95% confidence level. As can be deduced from this figure, the precision of the calorimeter is almost constant and it does not depend on the temperature.

Indium tests

To check the accuracy of the instrument when the sample cell is pressurized to 4.0 MPa, three calorimetric tests (under the continuous heating conditions reported in Table 1) were performed with indium (initial sample mass: 0.2506 ± 0.0010 g). Indium is a reference material which is particularly suitable for calibration purposes at pressures above atmospheric, because the pressure dependence of both the melting temperature and the heat of fusion of indium have been experimentally determined by high pressure dilatometry.[31, 32] The melting temperature of indium was used to check the temperature indicated by the instrument, while the heat of fusion of this metal was used to verify the heat (enthalpy) signal at 4.0 MPa.

Figure 5 shows the calorimetric curve for a representative experiment performed with indium. The net heat flow displayed in the figure was determined by subtracting the average heat flow corresponding to the blank tests from the experimental total heat flow. The enthalpy of fusion can be easily determined from the area of the DSC peak. The onset temperature has been considered as the experimental melting point following the suggestions of Ledru and coworkers.[31]

The reference values for the indium were taken from the work of Hohne and coworkers[32], where both melting point and fusion enthalpy at a given pressure value can be estimated using the following empirical equations:

$$T_{fus} = T_{fus}^{0} + 0.0507\,p \tag{1}$$

$$\Delta_{fus}H = \Delta_{fus}H^{0} + 3.3\times10^{-3}\,p - 2.6\times10^{-7}\,p^{2} \tag{2}$$

with pressure p in MPa (in this work, p = 4.0 MPa). $T_{fus}{}^{0}$ = 429.75 K and $\Delta_{fus}H^{0}$ = 28.62 J g^{-1} correspond to the reference values at atmospheric pressure.[31]

Table 2 shows the results obtained for the indium samples. As can be deduced from the data reported, the agreement with the reference values is excellent, especially for the enthalpy values.

Sapphire test

Despite the fact that the Tian-Calvet calorimeter was electrically calibrated by the manufacturer using a Joule-effect calibration cell, a DSC run was performed with synthetic sapphire (SRM 720 from NIST) to verify the accuracy of the Joule-effect calibration. The use of synthetic sapphire (α-aluminum oxide or corundum) as reference material is a common practice in the research community.[33–35] The sapphire run was performed at 0.1 MPa, under continuous heating conditions (see Table 1), using a sample mass of 15.8984 g. Figure 6 shows the differences between the experimental heat capacity values (on molar basis) obtained in the present work with those calculated using the following equation, which is reported in the NIST certificate:

$$(H_T - H_{273.15})/J\ mol^{-1} = \frac{6.6253\times10^{7}}{(T/K)^2} - \frac{4.54238\times10^{6}}{(T/K)} - 5.475599\times10^{4}\ln(T/K) + 2.5819702\times10^{5} + 2.574076\times10^{2}(T/K) - 8.57516\times10^{-2}(T/K)^2 + 4.299063\times10^{-5}(T/K)^3 - 1.15192\times10^{-8}(T/K)^4 + 1.26351\times10^{-12}(T/K)^5 \quad (3)$$

The differences displayed in Figure 6 are consistent with results reported in previous studies[24, 35] and are within the range of accuracy (± 1%) suggested by the IUPAC in a recent technical report.[33]

The general procedure followed to obtain the experimental value of heat capacity, at a given temperature, from the heat flow signal is described in detail in the next section.

Data processing

Determination of heat capacity from the DSC signal

For each calorimetric run, more than 10000 heat-flow data points are recorded (temperature, heat flow, and time). Obviously, it is not possible to calculate heat capacities for each data point because it is not possible to reach equilibrium during the short-time temperature increase. From experimental DSC curves, the specific heat of pure water was calculated according to the following expression:

$$C_p^{\exp} = \frac{I\times10^{-3}}{m(T_2 - T_1)} \quad (4)$$

Where C_p^{exp} corresponds to the uncorrected heat capacity value, I (in mJ) is the integrated area of the net heat flow (with subtraction of blank signal) within the range (T_1–T_2). The range length was 1 K in all cases and, obviously, the heat capacity value calculated using equation 4 corresponds to the average value at the average temperature (T_{avg}). Figure 7 shows an example of experimental DSC curves (obtained for sapphire at 0.1 MPa using the continuous heating regime) in order to provide a better understanding of the C_p^{exp} estimation process.

The estimation of the I value for a given temperature range involves a linear interpolation of the baseline by joining (with a straight line) the isothermal starting and ending net-heat-flow signals. This interpolation procedure is commonly adopted in the literature (see, for instance, the works of Cerdeiriña and coworkers[26] and Vizcaíno and coworkers[36]). Despite of the fact that several authors (such as Hemminger and Sarge[37]) have reported interesting methodologies to predict the shape of the baseline under a peak, a more sophisticated (but not necessarily more accurate) interpolation of the baseline for the entire measuring range using a mathematical function (i.e., an exponential function) seems inappropriate for the type of experiments reported here as a consequence of the long duration of experiments (from 28 to 34 hours) and the specific shape of the DSC curves.

Figure 8 shows two DSC experimental curves obtained for pure water, at a sample pressure of 4.0 MPa, for the two types of heating programs (continuous and stepwise) used in the present study. In both cases, the interpolated baseline differs from the ideal zero-constant baseline. In other words, an offset drift is observed. The offset can be defined as the deviation from the expected zero value of the net heat flow signal at the end of an isothermal period (Figure 8a shows an example). This fact could be related to the liquid nitrogen cooling process. Small fluctuations of the liquid nitrogen flow can slightly affect the temperature distribution in the calorimeter block and, consequently, the value of the heat flow signal measured by the instrument during an isothermal period can be slightly different for two successive experiments. However, this fact does not affect the accuracy in the calculation of the I values, because this process takes into account the baseline position for each temperature range evaluated according to the following equation:

$$I = \int_{t_1}^{t_2} NHF \; dt + \frac{1}{2}(b_1 + b_2)(t_2 - t_1) \tag{5}$$

where NHF is the net heat flow signal (in mW), t_1 and t_2 are the times corresponding to the initial (T_{avg}–0.5) and final (T_{avg}+0.5) temperatures, respectively; and b_1 and b_2 are the initial and final values of the interpolated baseline (for the temperature range evaluated), respectively. In

this way, the second term of the equation corrects the value of the numerical integral (which is mathematically calculated assuming a zero-constant baseline) by adding or subtracting an additional area, which is a function of the baseline position. Figure 9 graphically summarizes the procedure followed to calculate the *I* values.

For experiments performed at 4.0 MPa using the continuous heating program, *I* values have been calculated for average temperatures ranging from 298.15 K to 462.15 K in steps of 5 K. In the case of experiments with pure water at 0.1 MPa, the values of the integrated area of the *NHF* signal have been calculated for average temperatures ranging from 313.15 K to 353.15 K (also in steps of 5 K). Figure 10a shows an example of DSC curve obtained at 0.1 MPa using the continuous heating program.

Regarding the measurements performed at 4.0 MPa using the stepwise heating program reported in Table 1, Figure 8b displays the temporal evolution of both the temperature and the net heat flow. As has been mentioned above, the stepwise method can provide a higher degree of accuracy than the continuous heating method. Between two temperature isotherms, the thermal effect corresponding to the sample being heated is integrated. This method could allow the sample to reach thermal equilibrium after a temperature step. However, the main drawback of the stepwise heating program is the long time required for experiments. In this context, the relaxation time between two isotherms is a critical parameter. In this work, a relaxation time of 1800 s was selected in order to achieve a compromise between time required and accuracy. From analyzing Figure 8b, it is interesting to note that the sample temperature does not reach a stable set point during the isothermal holding stages. This fact could indicate that the selected relaxation time is too short and, consequently, the sample temperature does not remain constant during this period. Nevertheless, the heat flow curve shows a relatively good evolution. In other words, the selected relaxation time (1800 s) is enough to obtain a reasonably stabilized heat flow for each temperature step. In this sense, Merzlyakov and Schick[38] stated that it is not necessary to record the heat flow over the whole relaxation time when a series of similar step measurements with similar peak shapes are performed.

Taking into account the above-mentioned considerations for the experiments performed at 4.0 MPa using the stepwise heating program, *I* values have been calculated for the following average temperatures: 298.15, 326.65, 345.65, 366.65, 385.65, 406.65, 425.66, 446.65, and 465.65 K. These values correspond to the almost flat parts of the heat flow curve (see Figure 8b). For experiments conducted at 0.1 MPa, calculations were performed for the following average temperatures: 313.15, 333.15, and 353.15 K. Figure 10b displays an example of DSC curve

obtained at 0.1 MPa using the stepwise heating program, the parameters of which are reported in Table 1.

Correction due to the different amount of nitrogen contained in the cell

The preliminary estimated values of I (using equation 5) need to be corrected in order to include the effect related to different amounts of inert gas initially contained in the calorimetric sample cell. In this sense, the energy variations due to this effect can be estimated, for each temperature increment (T_2-T_1), as follows:

ΔQ = [*heat absorbed by N_2 contained in the empty sample cell (blank test)*] – [*heat absorbed by N_2 contained in the partially filled sample cell*] (6)

To perform the calculations required to estimate the values of ΔQ, the temperature-dependent values of density, for H_2O (liq), and both density and heat capacity, for N_2 (g), were taken from the NIST Chemistry WebBook (http://webbook.nist.gov/chemistry/). Once the value of ΔQ is estimated, the corrected integrated area of the net heat flow signal, I', can be obtained by the following equation:

$$I' = I + \Delta Q \tag{7}$$

It is interesting to note that, using this approach, the corrected values of the integrated area (I') are higher than those initially estimated (I). This is expected because the net heat flow is calculated by subtracting from the total heat flow the average heat flow corresponding to the blank tests (performed at identical operating conditions). In this way, the *NHF* values are underestimated due to the fact that the empty-cell heat flow values are obtained for a higher amount of nitrogen contained in the calorimetric cell.

In practice, and as might be expected, the differences between uncorrected and corrected integrated areas are relatively small. For experiments conducted with pure water at 4.0 MPa, differences ranged from 0.60% (at 465.65 K) to 1.15% (at 298.15 K); whereas for atmospheric pressure measurements, differences were negligible.

Correction due to the vapor contribution

The effect of a second gas (N_2) on the vapor pressure of a liquid (H_2O) at total constant pressure (p), assuming that the gaseous phase behaves as a perfect mixture, can be mathematically expressed as follows[39]:

$$\ln\left(\frac{p_{\alpha_2}}{p_{\alpha_1}}\right) = \frac{-\Delta_{vap}H}{R}\left(\frac{1}{T_2} - \frac{1}{T_1}\right) \tag{8}$$

where p_α denotes the vapor pressure of water at the total pressure p (0.1 or 4.0 MPa in the present work) and $\Delta_{vap}H$ is the enthalpy of the vaporization of water at the total pressure p (40.660 kJ mol^{-1} at 0.1 MPa and 30.868 kJ mol^{-1} at 4.0 MPa, assuming the IAPWS-95 formulation). This approximation form of the Clausius-Clapeyron equation becomes accurate if a second gas is present, insoluble or almost insoluble in the condensed phase, in such a way that the total pressure is constant.[39] Regarding the solubility of nitrogen in liquid water in the range of operating conditions considered in the present work, very low solute mass fractions were calculated using the regression equations reported by Battino and coworkers[40] (a highest value of 0.0000832 was obtained at 465.65 K and 4.0 MPa). For this reason, the contribution of the heat of solution of N_2 into water can be considered as negligible in the present application.

The starting value of p_α at total constant pressure (p) and $T_{l,initial}$ (the lower bound for the first temperature range evaluated: 297.65 K for experiments conducted at 4.0 MPa and 312.65 K for those conducted under atmospheric pressure) can be estimated by means of the following expression, which is closely related to equation 8 and only applicable at constant temperature[39]:

$$\ln\left(\frac{p_\alpha}{p^*}\right) = \frac{v_\beta}{RT_{1,initial}}(p - p_\alpha) \tag{9}$$

where p^* is the vapor pressure of pure water under its own pressure only (which is obtained from the IAPWS-95 steam tables for saturated steam at $T_{l,initial}$), and v_β is the molar volume of liquid water at the total constant pressure and $T_{l,initial}$ (deduced from the NIST Chemistry WebBook). Once the starting value of p_α at $T_{l,initial}$ is estimated using equation 9, the values of this variable at a given temperature can be calculated using equation 8. At this point, the amount of vapor can be easily determined for each temperature assuming a vapor space equal to the difference between the volume cell (8.5 cm^3) and the liquid volume (which is temperature dependent). On the other hand, the validity of equations 8 and 9 is based on the assumption that the water vapor obeys the ideal gas law. In this sense, the values of p_α and Z (compressibility factor) at the highest temperature (465.65 K) and at 4.0 MPa for water vapor are 285.5 kPa and 0.9918, respectively. On the basis of these data, ideal gas behavior can be assumed and, consequently, equations 8 and 9 can be used for the purpose of the present study.

Taking into account everything mentioned above, the corrected average heat capacity value for pure water (at the average temperature), C_p^{corr}, was calculated according to the following expression:

$$C_p^{corr} = \frac{I' - m_V C_{p,v}(T_2 - T_1) - \Delta m_V \Delta_{vap} H}{m_L (T_2 - T_1)} \quad (10)$$

where m_V and m_L correspond to the average mass over the temperature interval of vapor and liquid, respectively; and $C_{p,v}$ is the average heat capacity of the water vapor (at p_α), which was obtained from the steam tables based on the IAPWS-95 formulation. The value of Δm_V corresponds to the water vapor mass gain in the temperature range (T_1–T_2).

Results and Discussion

Tables 3 and 4 report the results of all experiments performed at 0.1 MPa under both continuous and stepwise heating conditions, respectively. An examination of these results indicates that some disagreement between calculated (average C_p^{corr} values derived from the three experiments at 0.1 K min^{-1} with confidence intervals of 95% according to a t-distribution) and reference (IAPWS-95) values exists, especially at the highest operating temperature (353.15 K). However, the differences observed are relatively small and can be attributed to the unavoidable uncertainty associated to any measurement. In fact, Figure 11 shows that the discrepancies observed at these temperatures and 0.1 MPa, for the heat capacity values reported here (the average C_p^{corr} values from experiments conducted at a continuous heating rate of 0.10 K min^{-1}), are of similar order as those reported in some previous studies[23, 27, 41] for the same temperature range. Lourenço and coworkers[23] measured the heat capacity of water in a Tian-Calvet calorimeter (Setaram model DSC-111) using closed stainless steel crucibles under stepwise heating conditions. Diedrichs and Gmehling[27] used a differential scanning calorimeter (TA Instruments model DSC Q100, not calibrated by Joule-effect) with closed aluminum crucibles (sample mass is in the range of 5–10 mg) using a three-step method (sapphire as a reference substance) under stepwise heating conditions (heating rate: 20 K min^{-1}). Finally, Chiu and coworkers[41] determined the heat capacity of pure water (sample mass is in the range of 15–20 mg) using a TA Instruments DSC (model DSC-2010, not calibrated by Joule-effect) and an experimental procedure similar to that followed by Diedrichs and Gmehling[27]. As shown in Table 4, a maximum disagreement of 0.75 % (at 353.15 K) is observed for the results of the present study. Although this difference may seem somewhat large, it should be noted that Lourenço and coworkers reported an estimated uncertainty of 1.1% at a 95% confidence level for their measurements, which were performed using a Tian-Calvet differential scanning calorimeter (an experimental device which uses the same principle as that used in this work). This relatively good

agreement, in combination with the results obtained from the sapphire test, could confirm the accuracy of the measuring instrument used in the present study.

A comparison between Table 3 and Table 4 reveals reasonably good agreement between the results obtained from experiments subjected to a stepwise heating program with those obtained using a continuous heating program. The observed small differences could be attributed to the inherently better accuracy of the stepwise method. Nevertheless, the relatively short relaxation time selected in this study for the stepwise heating program could be a potential source of uncertainty. For this reason, further experiments using longer relaxation times will probably be needed in the future in order to estimate the effect of this variable on the heat flow results.

Table 3 also reports the results obtained for an additional experiment (exp#13), which was conducted at 0.15 K min^{-1} (the heating rate selected for all experiments performed at 4.0 MPa) instead of 0.10 K min^{-1}. In light of the very small differences in the heat capacity between experiments carried out at different heating rates, it seems reasonable to suggest that the accuracy of the calorimeter is not adversely affected when the heating rate increases from 0.10 to 0.15 K min^{-1}.

Regarding the experiments performed at 4.0 MPa, unexpected results were obtained for the specific heat capacity of water. For the experiments performed under continuous heating conditions, Table 5 reports the calculated C_p^{corr} values (average values derived from the three experiments and confidence intervals of 95% according to a t-distribution) and the reference ones reported by Wagner and Pruss[1] at 4.0 MPa. The differences between the reference values (IAPWS-95) and those obtained in the present study become significantly greater as temperature increases (from 5.34% at 298.15 K to 25.36% at 463.15 K). On the other hand, Table 5 also reports the experimental (uncorrected) heat capacity values (C_p^{exp}). As can be deduced by comparing the appropriate numbers in Table 5, the correction approach adopted in the present study makes a relatively small contribution to the disagreement between the present data and that reported by Wagner and Pruss.[1]

The experimental results obtained for pure water at 4.0 MPa using the stepwise heating method (reported in Table 6 for both uncorrected and corrected heat capacities) are also considerably higher than the reference values (IAPWS-95[1]). However, the results reported in Table 6 are slightly higher than those obtained using the continuous heating program (and reported in Table 5) for temperatures ranging from 325 to 410 K (a comparison of the heat capacity results is displayed in Figure 12). This fact could be attributed to the expected lower accuracy of the continuous heating regime.

Nevertheless and as a general remark, the overall results obtained at 4.0 MPa seem to indicate that, for the type of calorimeter used in the present study, the use of a continuous heating program (which requires less experimental time) allows a reasonably accurate measurement of the specific heat capacity. However, and as has been noted previously, further experiments using a stepwise heating program with longer relaxation times will probably be needed to confirm the validity of the continuous heating mode.

Figure 13 shows additional results obtained at two intermediate pressures (0.5 MPa and 3.3 MPa). The data at 0.5 MPa were determined in the Setaram laboratory (Lyon, France) using a C80 calorimeter (a Tian-Calvet differential scanning calorimeter, which works on the same design principle as the BT2.15) with a high pressure gas circulation cell under continuous heating rate conditions (0.2 K min^{-1}), while the data at 3.3 MPa were obtained by the authors using the experimental devices and procedures described in the present study. Although the additional data are not strictly comparable because they are based on single measurements, the differences in heat capacity between experimental and reference values at 0.5 and 3.3 MPa are also important.

To highlight the effect of the value of the specific heat capacity of water on the estimation of the apparent molar heat capacity (C_p^{ϕ}) of a given electrolyte (i.e., NaCl), the experimental data measured by Gates and coworkers[42] at 448.15 K and 4.0 MPa by means of a Picker-type flow calorimeter have been reevaluated using the C_p values of pure water reported here.

According to several researchers[43-46], the apparent molar heat capacity (in J mol^{-1} K^{-1}) for binary systems can be written as a function of experimental heat capacity values as follows:

$$C_p^{\phi} = M\ C_{p,s} + \left[\frac{1000\left(C_{p,s} - C_{p,w}\right)}{m_B}\right] \tag{11}$$

where M is the molecular weight of the solute, m_B is the molality of the solute, $C_{p,s}$ is the specific heat capacity of the solution (experimental value), and $C_{p,w}$ is the specific heat capacity of pure water, respectively. It can be deduced from the second term in equation 11 that the final value of Cp^{ϕ} is particularly sensitive to the difference ($C_{p,s} - C_{p,w}$), and that this difference is amplified increasingly as m_B decreases because of the factor ($1/m_B$). Figure 14 displays the apparent molar heat capacity of NaCl(aq) as a function of molality for data reported by Gates and coworkers[42] at 448.15 K and 4.0 MPa assuming the IAPWS-95 formulation for the heat capacity of water. In the same figure, the recalculated Cp^{ϕ} values assuming the $C_{p,w}$ value reported in Table 5 (5.214 J g^{-1} K^{-1}) are also shown. As can be deduced from Figure 14, a change of the heat capacity value of water from 4.391 J g^{-1} K^{-1} (IAPWS-95) to 5.214 J g^{-1} K^{-1} (this work) causes a

dramatic effect on the calculation of the apparent molar heat capacity and, consequently, on the estimation of thermodynamic properties of aqueous electrolytes at a given pressure and temperature.

Conclusions

The calorimetric results obtained for the specific heat capacity of pure water at 4.0 MPa are clearly in disagreement with the values obtained using the IAPWS-95 formulation, especially at high temperatures. On the basis of these findings, the authors would emphasize the need for the research community to revisit the calorimetric measurements of the heat capacity of liquid water at high temperatures and pressures.

The results reported here should be confirmed independently. The stepwise heating program adopted in the present study involves a certain degree of uncertainty because the experimental time consumed between two isotherms is not enough to completely stabilize the heat flow signal. In addition, the theoretical correction of the vapor contribution, by means of an approximate form of the Clausius-Clapeyron equation (eq. 8), might add a certain level of uncertainty to the heat capacity values reported in the present study. Nevertheless, this correction accounts for only a small portion of the disagreement between the present data and that reported by Wagner and Pruss.[1]

Conducting more extensive experimental studies, focused on the measurement of the specific heat of pure water at different pressures and temperatures, should be a priority for the international research community in order to confirm the trends found in this work. In the short term, it seems advisable to perform a round-robin study, for the measurement of the specific heat capacity of pure water, involving several different types of calorimeters (and cells) and different heat flow quantification techniques.

Acknowledgement

The authors acknowledge and thank the helpful comments and suggestions of Ryan J. Kurasaki (HNEI). The authors would also like to thank Dr. Luc Benoist for his experiments performed at the application laboratory of Setaram (Lyon, France). JJM acknowledges the financial support provided by the European Social Found and the Spanish Ministry of Science and Innovation ("Juan de la Cierva" contract and "José Castillejo" mobility program). He also thanks Dr. Gloria Gea (University of Zaragoza) for her assistance in statistical analysis. MJA acknowledges support by the National Science Foundation (Award No. CBET08-28006), the Office of Naval Research under the Hawaii Energy and Environmental Technologies (HEET) initiative, and the Coral Industries Endowment of the University of Hawaii. He thanks Dr. Maria Burka (NSF) for her continuing interest in carbon fuel cell research, and his colleagues in HNEI for their encouragement.

Nomenclature

b_1	*Value of the interpolated baseline corresponding to T_1 (mW)*
b_2	*Value of the interpolated baseline corresponding to T_2 (mW)*
C_p	*Heat capacity (J g^{-1} K^{-1})*
C_p^{exp}	*Experimental (uncorrected) heat capacity value (J g^{-1} K^{-1})*
C_p^{corr}	*Corrected heat capacity value (J g^{-1} K^{-1})*
$C_{p,s}$	*Specific heat capacity of an aqueous solution (J g^{-1} K^{-1})*
$C_{p,v}$	*Average heat capacity of the water vapor (J g^{-1} K^{-1})*
$C_{p,w}$	*Specific heat capacity of water in equation 11 (J g^{-1} K^{-1})*
$C_p^{ø}$	*Apparent molar heat capacity (J mol^{-1} K^{-1})*
$H_{273.15}$	*Enthalpy of synthetic sapphire at 273.15 K (J mol^{-1})*
H_T	*Enthalpy of synthetic sapphire at a given temperature (J mol^{-1})*
I	*Integrated area of the net heat flow signal, within the range (T_1–T_2), (mJ)*
I'	*Corrected integrated area of the net heat flow signal, within the range (T_1–T_2), (mJ)*
M	*Molecular weight of the solute (g mol^{-1})*
m	*Sample mass (g)*
m_B	*Molality of the solute (mol kg^{-1})*
m_L	*Average mass of water liquid contained in the cell (g)*
m_V	*Average mass of water vapor contained in the cell (g)*
NHF	*Net heat flow signal (mW)*
p	*Total pressure (Pa)*
p^*	*Vapor pressure of pure water (Pa)*
p_α	*Vapor pressure of pure water at the total pressure p (Pa)*
T	*Temperature (K)*
T_0	*Initial temperature (K)*
T_1	*Lower limit of a predetermined temperature range (K)*
$T_{1,initial}$	*Lower limit of the first temperature range evaluated (K)*
T_2	*Upper limit of a predetermined temperature range (K)*
T_{avg}	*Average temperature value between T_1 and T_2 (K)*
T_{exp}	*Experimental melting point of indium (K)*
T_f	*Final temperature (K)*

T_{fus} *Theoretical melting point of indium (K)*

T_{fus}^{0} *Theoretical melting point of indium at atmospheric pressure (K)*

t *Measuring time (s)*

t_1 *Measuring time corresponding to T_1 (s)*

t_2 *Measuring time corresponding to T_2 (s)*

Z *Compressibility factor (-)*

Greek Symbols

β *Heating rate (K min^{-1})*

$\Delta_{exp}H$ *Experimental enthalpy of fusion of indium (J g^{-1})*

$\Delta_{fus}H$ *Theoretical enthalpy of fusion of indium (J g^{-1})*

$\Delta_{fus}H^{0}$ *Theoretical enthalpy of fusion of indium at atmospheric pressure (J g^{-1})*

$\Delta_{vap}H$ *Enthalpy of vaporization of water (J g^{-1})*

ΔQ *Correction due to the different amount of nitrogen contained in the cell (J)*

v_β *Molar volume of liquid water (m^3 mol^{-1})*

Subscripts

exp *experimental*

ref *reference*

Superscripts

exp *experimental (uncorrected)*

corr *corrected*

Acronyms

DSC *Differential Scanning Calorimetry*

IAPWS *International Association for the Properties of Water and Steam*

ITC *International Temperature Scale*

NIST *National Institute of Standards and Technology*

SRM *Standard Reference Material*

Literature Cited

(1) Wagner, W.; Pruss, A. The IAPWS formulation 1995 for the thermodynamic properties of ordinary water substance for general and scientific use. *J. Phys. Chem. Ref. Data* **2002***, 31*, 387–535.

(2) Nunoura, T.; Dowaki, K.; Fushimi, C.; Allen, S.; Meszaros, E.; Antal, M. J. Performance of a First-Generation, Aqueous-Alkaline Biocarbon Fuel Cell. *Ind. Eng. Chem. Res.* **2007***, 46*, 734–744.

(3) Antal, M. J.; Nihous, G. C. Thermodynamics of an Aqueous-Alkaline/Carbonate Carbon Fuel Cell. *Ind. Eng. Chem. Res.* **2008***, 47*, 2442–2448.

(4) Koschel, D.; Coxam, J.; Rodier, L.; Majer, V. Enthalpy and solubility data of CO_2 in water and NaCl(aq) at conditions of interest for geological sequestration. *Fluid Phase Equilib.* **2006***, 247*, 107–120.

(5) Pruess, K.; Spycher, N. ECO2N – A fluid property module for the TOUGH2 code for studies of CO_2 storage in saline aquifers. *Energy Conv. Manage.* **2007***, 48*, 1761–1767.

(6) Sirota, A. M.; Mal'tsev, B. K. Experimental investigation of the heat capacity of water at 1–500 ºC and to pressures of 500 kbar/cm^2. *Teploenergetika* **1959***, 6*, 7.

(7) Angell, C. A.; Sichina, W. J.; Oguni, M. Heat capacity of water at extremes of supercooling and superheating. *J. Phys. Chem.* **1982***, 86*, 998–1002.

(8) Czarnota, I. Heat capacity of water at high pressure. *High Temp.-High Press.* **1984***, 16*, 295–302.

(9) Kestin, J.; Sengers, J. V. New International Formulations for the Thermodynamic Properties of Light and Heavy Water. *J. Phys. Chem. Ref. Data* **1986***, 15*, 305–320.

(10) Archer, D. G.; Carter, R. W. Thermodynamic Properties of the NaCl + H_2O System. 4. Heat Capacities of H_2O and NaCl(aq) in Cold-Stable and Supercooled States. *J. Phys. Chem. B* **2000***, 104*, 8563–8584.

(11) Kuznetsov, M. A.; Lazarev, S. I. A modernized calorimeter for measuring the isobaric heat capacity of hydrocarbons by a continuous-flow method in the critical region. *Meas. Tech.* **2005**, *48*, 798–804.

(12) Picker, P.; Leduc, P.-A.; Philip, P. R.; Desnoyers, J. E. Heat capacity measurement by flow calorimetry. *J. Chem. Thermodyn.* **1971**, *3*, 631–641.

(13) Rogers, P. S. Z.; Duffy, C. J. Comparison of calibration methods for flow heat-capacity calorimeters and heat capacities of concentrated NaCl(aq) to 598 K. *J. Chem. Thermodyn.* **1989**, *21*, 595–614.

(14) Carter, R. W.; Wood, R. H. Calibration and sample-measurement techniques for flow heat-capacity calorimeters. *J. Chem. Thermodyn.* **1991**, *23*, 1037–1056.

(15) Archer, D. G. Thermodynamic Properties of the NaCl + H_2O System II. Thermodynamic Properties of NaCl(aq), NaCl·$2H_2O$(cr), and Phase Equilibria. *J. Phys. Chem. Ref. Data* **1992**, *21*, 793–829.

(16) Hnedkovsky, L.; Hynek, V.; Majer, V.; Wood, R. H. A new version of differential flow heat capacity calorimeter; tests of heat loss corrections and heat capacities of aqueous NaCl from T = **300** K to T = 623 K. *J. Chem. Thermodyn.* **2002**, *34*, 755–782.

(17) Desnoyers, J. E.; de Visser, C.; Perron, G.; Picker, P. Reexamination of the Heat Capacities Obtained by Flow Microcalorimetry. Recommendation for the Use of a Chemical Standard. *J. Solution Chem.* **1976***, 5*, 605–616.

(18) Ballerat-Busserolles, K.; Origlia, M. L.; Woolley, E. M. Calibration of a fixed-cell temperature-scanning calorimeter to measure precise solution heat capacities from 275 to 398 K at 0.35 MPa. *Thermochim. Acta* **2000***, 347*, 3–7.

(19) Jones, J. S.; Ziemer, S. P.; Brown, B. R.; Woolley, E. M. Apparent molar volumes and apparent molar heat capacities of aqueous magnesium nitrate, strontium nitrate, and manganese nitrate at temperatures from 278.15 K to 393.15 K and at the pressure 0.35 MPa. *J. Chem. Thermodyn.* **2007***, 39*, 550–560.

(20) Magalhaes, M. C. F.; Konigsberger, E.; May, P. M.; Hefter, G. Heat Capacities of Concentrated Aqueous Solutions of Sodium Sulfate, Sodium Carbonate, and Sodium Hydroxide at 25 °C. *J. Chem. Eng. Data* **2002***, 47*, 590–598.

(21) Patterson, B. A.; Call, T. G.; Jardine, J. J.; Origlia-Luster, M. L.; Woolley, E. M. Thermodynamics for ionization of water at temperatures from 278.15 K to 393.15 K and at the pressure 0.35 MPa: apparent molar volumes of aqueous KCl, KOH, and NaOH and apparent molar heat capacities of aqueous HCl, KCl, KOH, and NaOH. *J. Chem. Thermodyn.* **2001***, 33*, 1237–1262.

(22) Schrödle, S.; Königsberger, E.; May, P. M.; Hefter, G. Heat capacities of aqueous solutions of sodium hydroxide and water ionization up to 300 C at 10 MPa. *Geochim. Cosmochim. Acta* **2008***, 72*, 3124–3138.

(23) Lourenço, M. J. V.; Santos, F. J. V.; Ramires, M. L. V.; de Castro, C. A. N. Isobaric specific heat capacity of water and aqueous cesium chloride solutions for temperatures between 298 K and 370 K at p = 0.1 MPa. *J. Chem. Thermodyn.* **2006***, 38*, 970–974.

(24) Sampaio, M. O.; Nieto de Castro, C. A. Heat capacitiy of liquid terpenes. *Fluid Phase Equilib.* **1998***, 150–151*, 789–796.

(25) Woolley, E. M. A new tool for an old job: Using fixed cell scanning calorimetry to investigate dilute aqueous solutions. *J. Chem. Thermodyn.* **2007***, 39*, 1300–1317.

(26) Cerdeiriña, C. A.; Míguez, J. A.; Carballo, E.; Tovar, C. A.; de la Puente, E.; Romaní, L. Highly precise determination of the heat capacity of liquids by DSC: calibration and measurement. *Thermochim. Acta* **2000***, 347*, 37–44.

(27) Diedrichs, A.; Gmehling, J. Measurement of heat capacities of ionic liquids by differential scanning calorimetry. *Fluid Phase Equilib.* **2006**, *244*, 68–77.

(28) Paramo, R.; Zouine, M.; Casanova, C. New Batch Cells Adapted To Measure Saturated Heat Capacities of Liquids. *J. Chem. Eng. Data* **2002***, 47*, 441–448.

(29) Zhang, K.; Hawrylak, B.; Palepu, R.; Tremaine, P. R. Thermodynamics of aqueous amines: excess molar heat capacities, volumes, and expansibilities of {water + methyldiethanolamine (MDEA)} and {water + 2-amino-2-methyl-1-propanol (AMP)}. *J. Chem. Thermodyn.* **2002***, 34*, 679–710.

(30) Burdick, R. K.; Borror, C. M.; Montgomery, D. C. *Design and analysis of gauge R&R studies: making decisions with confidence intervals in random and mixed ANOVA models*. Society for Industrial Applied Mathematics: Philadelphia, 2005.

(31) Ledru, J.; Imrie, C. T.; Hutchinson, J. M.; Höhne, G. W. H. High pressure differential scanning calorimetry: Aspects of calibration. *Thermochim. Acta* **2006***, 446*, 66–72.

(32) Höhne, G. W. H.; Dollhopf, W.; Blankenhorn, K.; Mayr, P. U. On the pressure dependence of the heat of fusion and melting temperature of indium. *Thermochim. Acta* **1996***, 273*, 17–24.

(33) Della Gatta, G.; Richardson, M. J.; Sarge, S. M.; Stolen, S. Standards, calibration, and guidelines in microcalorimetry. Part 2: calibration standards for differential scanning calorimetry (IUPAC Technical Report). *Pure Appl. Chem.* **2006**, *78*, 1455–1476.

(34) Mundhwa, M.; Elmahmudi, S.; Maham, Y.; Henni, A. Molar Heat Capacity of Aqueous Sulfolane, 4-Formylmorpholine, 1-Methyl-2-pyrrolidinone, and Triethylene Glycol Dimethyl Ether Solutions from (303.15 to 353.15) K. *J. Chem. Eng. Data* **2009,** *54,* 2895–2901.

(35) Zhao, X.; Liu, Z.; Chen, Z. Heat Capacities of Five Mixtures and Emulsion of Buna-S. *J. Chem. Eng. Data* **2006,** *51,* 867-870.

(36) Vizcaıno, P.; Rios, R. O.; Banchik, A. D. Hydrogen determinations in a zirconium based alloy with a DSC. *Thermochim. Acta* **2005**, *429*, 7–11.

(37) Hemminger, W. F.; Sarge, S. M. The baseline construction and its influence on the measurement of heat with differential scanning calorimeters. *J. Therm. Anal.* **1991***, 37*, 1455–1477.

(38) Merzlyakov, M.; Schick, C. Step response analysis in DSC — a fast way to generate heat capacity spectra. *Thermochim. Acta* **2001***, 380*, 5–12.

(39) Denbigh, K. G. *The principles of chemical equilibrium: with applications in chemistry and chemical engineering*; Cambridge University Press: New York, 1981.

(40) Battino, R.; Rettich, T. R.; Tominaga, T. The solubility of nitrogen and air in liquids. *J. Phys. Chem. Ref. Data* **1984***, 13*, 563–600.

(41) Chiu, L.-F.; Liu, H.-F.; Li, M.-H. Heat Capacity of Alkanolamines by Differential Scanning Calorimetry. *J. Chem. Eng. Data* **1999,** *44,* 631–636.

(42) Gates, J. A.; Tillett, D. M.; White, D. E.; Wood, R. H. Apparent molar heat capacities of aqueous NaCl solutions from 0.05 to 3.0 mol·kg^{-1}, 350 to 600 K, and 2 to 18 MPa *J. Chem. Thermodyn.* **1987**, *19*, 131–146.

(43) Hovey, J. K. Thermodynamics of Hydration of a 4+ Aqueous Ion: Partial Molar Heat Capacities and Volumes of Aqueous Thorium(IV) from 10 to 55 °C. *J. Phys. Chem. B* **1997***, 101,* 4321–4334.

(44) Saluja, P. P. S.; Jobe, D. J.; Leblanc, J. C.; Lemire, R. J. Apparent Molar Heat-Capacities and Volumes of Mixed Electrolytes - [NaCl(aq)+$CaCl_2$(aq)], [NaCl(aq)+$MgCl_2$(aq)], and [$CaCl_2$(aq)+$MgCl_2$(aq)]. *J. Chem. Eng. Data* **1995***, 40,* 398–406.

(45) Jones, J. S.; Ziemer, S. P.; Brown, B. R.; Woolley, E. M. Apparent molar volumes and apparent molar heat capacities of aqueous magnesium nitrate, strontium nitrate, and manganese nitrate at temperatures from 278.15 K to 393.15 K and at the pressure 0.35 MPa. *J. Chem. Thermodyn.* **2007***, 39,* 550–560.

(46) Manyà, J. J.; Antal, M. J. Review of the Apparent Molar Heat Capacities of NaCl(aq), HCl(aq), and NaOH(aq) and Their Representation Using the Pitzer Model at Temperatures from (298.15 to 493.15) K. *J. Chem. Eng. Data* **2009,** *54,* 2158–2169.

Table 1. Calorimeter heating programs used in the present study

	p = 0.1 MPa		p = 4.0 MPa	
Continuous heating regime	T_0 (K)	298.15	T_0 (K)	283.15
	Isothermal period at T_0 (s)	3600	Isothermal period at T_0 (s)	3600
	β (K min^{-1})	0.10	β (K min^{-1})	0.15
	T_f (K)	358.15	T_f (K)	473.15
	Experiments	#1, #2, #3	Experiments	#7, #8, #9
Stepwise heating regime	T_0 (K)	298.15	T_0 (K)	283.15
	Isothermal period at T_0 (s)	3600	Isothermal period at T_0 (s)	3600
	β (K min^{-1})	0.10	β (K min^{-1})	0.15
	Endpoint temperatures (K)	318.15, 338.15, and 358.15	Endpoint temperatures (K)	313.15, 333.15, 353.15, 373.15, 393.15, 413.15, 433.15, 453.15, and 473.15
	Relaxation time for each endpoint temperature (s)	3600	Relaxation time for each endpoint temperature (s)	1800
	Experiments	#4, #5; #6	Experiments	#10, #11, #12

Table 2. Results obtained from the indium tests

T_{fus} (K) calculated from eq. 1	T_{exp} (K)	Difference (K)
429.95	430.21 ± 0.11	–0.26
$\Delta_{fus}H$ (J g^{-1}) calculated from eq. 2	$\Delta_{exp}H$ (J g^{-1})	Difference (%)
28.633	28.638 ± 0.008	0.017

Table 3. Heat capacity values of liquid water obtained using the continuous heating program (p = 0.1 MPa)

	β = 0.10 K min^{-1} (exp #1, exp#2, and exp #3)				β = 0.15 K min^{-1} (exp #13)		
Temperature (K)	C_p^{exp} (J g^{-1} K^{-1})	C_p^{corr} (J g^{-1} K^{-1})	Reference values reported by Wagner and Pruss[1] (J g^{-1} K^{-1})	Difference between C_p^{corr} and reference values (%)	C_p^{exp} (J g^{-1} K^{-1})	C_p^{corr} (J g^{-1} K^{-1})	Difference between C_p^{corr} values obtained at 0.15 and 0.10 K min^{-1} (%)
313.15	4.172 ± 0.001	4.167 ± 0.001	4.182	–0.36	4.170	4.165	–0.04
318.15	4.177 ± 0.010	4.170 ± 0.012	4.183	–0.30	4.177	4.171	0.01
323.15	4.188 ± 0.012	4.180 ± 0.014	4.184	–0.10	4.194	4.186	0.16
328.15	4.181 ± 0.002	4.171 ± 0.001	4.186	–0.36	4.191	4.181	0.24
333.15	4.184 ± 0.006	4.172 ± 0.008	4.188	–0.38	4.197	4.186	0.32
338.15	4.188 ± 0.002	4.174 ± 0.006	4.190	–0.38	4.198	4.184	0.24
343.15	4.204 ± 0.002	4.186 ± 0.002	4.193	–0.16	4.206	4.189	0.07
348.15	4.212 ± 0.006	4.191 ± 0.011	4.196	–0.12	4.218	4.198	0.16
353.15	4.254 ± 0.005	4.230 ± 0.010	4.200	0.72	4.250	4.226	–0.08

Table 4. Heat capacity values of liquid water obtained using the stepwise heating program (p = 0.1 MPa)

Temperature (K)	C_p^{exp} (J g^{-1} K^{-1})	C_p^{corr} (J g^{-1} K^{-1})	Reference values reported by Wagner and Pruss[1] (J g^{-1} K^{-1})	Difference between C_p^{corr} and reference values (%)
313.15	4.173 ± 0.005	4.168 ± 0.005	4.182	–0.33
333.15	4.185 ± 0.007	4.184 ± 0.007	4.188	–0.11
353.15	4.254 ± 0.004	4.231 ± 0.003	4.200	0.75

Table 5. Heat capacity values of liquid water obtained using the continuous heating program (*p* = 4.0 MPa*)*

Temperature (K)	C_p^{exp} (J g^{-1} K^{-1})	C_p^{corr} (J g^{-1} K^{-1})	Reference values reported by Wagner and Pruss[1] (J g^{-1} K^{-1})	Difference with the reference values (%)	
				C_p^{exp}	C_p^{corr}
298.15	4.361 ± 0.004	4.407 ± 0.004	4.183	4.26	5.34
303.15	4.374 ± 0.011	4.417 ± 0.011	4.182	4.58	5.62
308.15	4.345 ± 0.014	4.386 ± 0.014	4.181	3.92	4.91
313.15	4.345 ± 0.013	4.384 ± 0.014	4.181	3.91	4.86
318.15	4.339 ± 0.004	4.377 ± 0.004	4.182	3.75	4.65
323.15	4.330 ± 0.004	4.366 ± 0.004	4.183	3.52	4.37
328.15	4.329 ± 0.005	4.362 ± 0.005	4.185	3.43	4.23
333.15	4.327 ± 0.007	4.359 ± 0.006	4.187	3.35	4.10
338.15	4.322 ± 0.019	4.351 ± 0.019	4.189	3.18	3.87
343.15	4.333 ± 0.016	4.360 ± 0.015	4.192	3.36	3.99
348.15	4.339 ± 0.007	4.363 ± 0.006	4.195	3.42	4.00
353.15	4.339 ± 0.013	4.361 ± 0.013	4.199	3.34	3.85
358.15	4.348 ± 0.011	4.367 ± 0.010	4.203	3.46	3.90
363.15	4.364 ± 0.008	4.380 ± 0.007	4.207	3.73	4.10
368.15	4.377 ± 0.012	4.390 ± 0.012	4.212	3.93	4.23
373.15	4.388 ± 0.018	4.397 ± 0.017	4.218	4.02	4.25
378.15	4.408 ± 0.011	4.414 ± 0.010	4.224	4.36	4.51
383.15	4.438 ± 0.008	4.441 ± 0.006	4.231	4.90	4.96
388.15	4.468 ± 0.015	4.466 ± 0.017	4.238	5.42	5.39
393.15	4.491 ± 0.008	4.486 ± 0.007	4.246	5.77	5.66
398.15	4.530 ± 0.018	4.521 ± 0.016	4.255	6.45	6.24
403.15	4.571 ± 0.005	4.558 ± 0.004	4.264	7.20	6.90
408.15	4.619 ± 0.011	4.602 ± 0.009	4.274	8.08	7.68
413.15	4.673 ± 0.006	4.652 ± 0.003	4.285	9.06	8.56
418.15	4.733 ± 0.017	4.707 ± 0.014	4.297	10.14	9.54
423.15	4.794 ± 0.015	4.763 ± 0.011	4.310	11.23	10.51
428.15	4.874 ± 0.016	4.838 ± 0.013	4.324	12.72	11.90
433.15	4.966 ± 0.004	4.925 ± 0.005	4.339	14.44	13.52
438.15	5.056 ± 0.008	5.011 ± 0.012	4.355	16.11	15.07
443.15	5.158 ± 0.017	5.108 ± 0.017	4.372	17.98	16.83
448.15	5.269 ± 0.014	5.214 ± 0.010	4.391	20.00	18.75
453.15	5.397 ± 0.020	5.337 ± 0.015	4.411	22.35	20.99
458.15	5.530 ± 0.012	5.465 ± 0.010	4.432	24.78	23.32
463.15	5.654 ± 0.041	5.585 ± 0.046	4.455	26.92	25.36

Table 6. Heat capacity values of liquid water obtained using the stepwise heating program (p = 4.0 MPa)

Temperature (K)	C_p^{exp} (J g^{-1} K^{-1})	C_p^{corr} (J g^{-1} K^{-1})	Reference values reported by Wagner and Pruss[1] (J g^{-1} K^{-1})	Difference with the reference values (%)	
				C_p^{exp}	C_p^{corr}
298.15	4.373 ± 0.026	4.413 ± 0.025	4.183	4.54	5.51
326.65	4.403 ± 0.027	4.438 ± 0.027	4.184	5.24	6.07
345.65	4.415 ± 0.015	4.441 ± 0.014	4.194	5.26	5.89
366.65	4.460 ± 0.059	4.475 ± 0.058	4.210	5.93	6.29
385.65	4.546 ± 0.009	4.549 ± 0.011	4.234	7.37	7.44
406.65	4.642 ± 0.001	4.629 ± 0.002	4.271	8.69	8.38
425.65	4.870 ± 0.043	4.841 ± 0.040	4.317	12.82	12.14
446.65	5.193 ± 0.038	5.144 ± 0.042	4.385	18.42	17.30
465.65	5.749 ± 0.037	5.682 ± 0.042	4.467	28.69	27.19

Caption for Figures

Figure 1. Experimental system: (a), block diagram (1, nitrogen; 2, tanks; 3, calorimeter; 4, vacuum pump; 5, liquid nitrogen; 6, gas inlet and outlet; 7, pressure transducer; 8, computer); and (b), sketch with the main items of the Tian-Calvet heat flow calorimeter.

Figure 2. Setaram High Pressure Gas Circulation cell (volume = 8.5 cm^3).

Figure 3. DSC curve for the blank tests performed using the continuous heating program at 4.0 MPa (solid line, blank test #1; dashed line, blank test #2; dotted line, blank test #3): (a), entire curve; and (b), zoom detail.

Figure 4. Results from the analysis of the measurement system variation: (a), Minitab output results from the crossed gage R&R study; and (b), interval plot for the means at 95% confidence level.

Figure 5. DSC curve for a representative indium test. The dashed line corresponds to the uncorrected heat flow signal, whereas the solid line corresponds to the net heat flow.

Figure 6. Differences, as a function of temperature, between experimental and reference values (NIST certificate) for specific heat capacity of synthetic sapphire at 0.1 MPa.

Figure 7. DSC curves for an experiment performed with sapphire at constant heating rate: (a) the thin solid line is the heat flow obtained for the blank test, and the bold solid line corresponds to the total heat flow; (b) the bold solid line is the net heat flow (which is obtained by subtracting the heat flow corresponding to the blank test from the total heat flow), the dotted line is the zero-constant baseline, and the shaded area is the integrated value of the net heat flow (assuming the zero-constant baseline) for a given average temperature (353.15 K).

Figure 8. Examples of DSC curves obtained for pure water at a sample pressure of 4.0 MPa: (a), exp#7 using the continuous heating program (see Table 1) and (b), exp#10 using the stepwise heating program (see Table 1).

Figure 9. A graphical example of the procedure followed to determine the *I* values (exp#7 at a given average temperature of 333.15 K). The area of the gray trapezoid represents the second term of equation 5.

Figure 10. Examples of DSC curves obtained for pure water at a sample pressure of 0.1 MPa: (a), exp#1 using the continuous heating program (see Table 1) and (b), exp#4 using the stepwise heating program (see Table 1).

Figure 11. Differences, as a function of temperature, between measured (■, this study using the continuous heating program at 0.10 K min^{-1}; ▲, Lourenço and coworkers[23]; ▽, Diedrichs and Gmehling[27]; ○, Chiu and coworkers[41]) and reference values (IAPWS-95) for specific heat capacity of pure water at 0.1 MPa.

Figure 12. Comparison of C_p^{corr} values for pure water at 4.0 MPa (▼, this study using the stepwise heating method; ○, this study using the continuous heating method; ■, data from IAPWS-95).

Figure 13. Differences between C_p^{corr} values obtained at different pressures (▼, at 4.0 MPa using the stepwise heating method; △, at 3.3 MPa using the stepwise heating method; ○, at 0.5 MPa from Setaram's lab using a C80 calorimeter under continuous heating rate conditions) and the corresponding reference values (black line, IAPWS-95 at 0.5 MPa; red line, IAPWS-95 at 3.3 MPa; blue line, IAPWS-95 at 4.0 MPa).

Figure 14. Apparent molar heat capacity of NaCl(aq) versus molality at 448.15 K and 4.0 MPa from measured $C_{p,s}$ data by Gates et al.[42] and: ■, the $C_{p,w}$ value assuming the IAPWS-95 formulation; △, the $C_{p,w}$ value reported in Table 5.

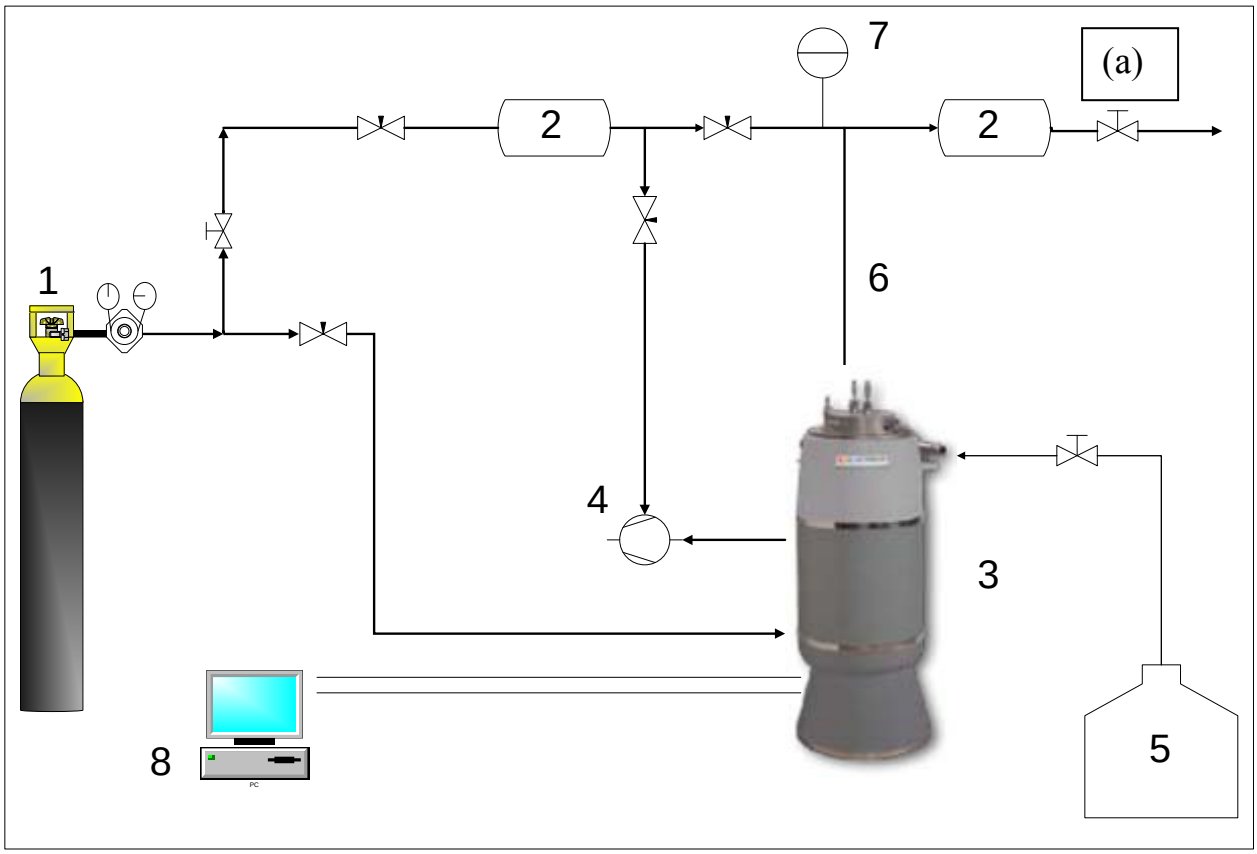

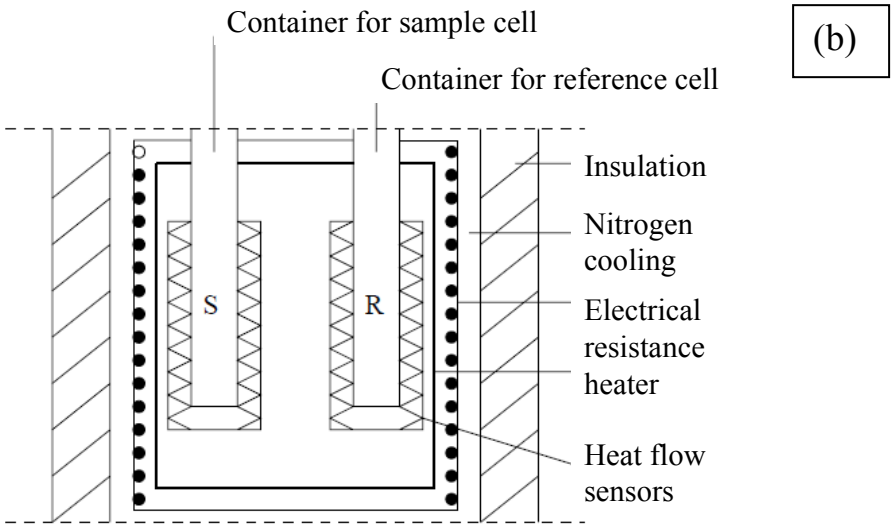

Figure 1. Experimental system: (a), block diagram (1, nitrogen; 2, tanks; 3, calorimeter; 4, vacuum pump; 5, liquid nitrogen; 6, gas inlet and outlet; 7, pressure transducer; 8, computer); and (b), sketch with the main items of the Tian-Calvet heat flow calorimeter.

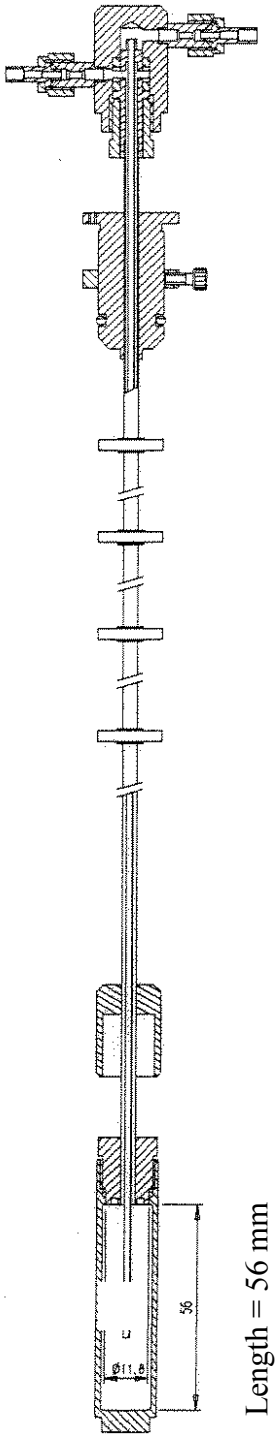

ID = 11.6 mm
Volume = 8.5 cm^3

Figure 2. Setaram High Pressure Gas Circulation cell (volume = 8.5 cm^3).

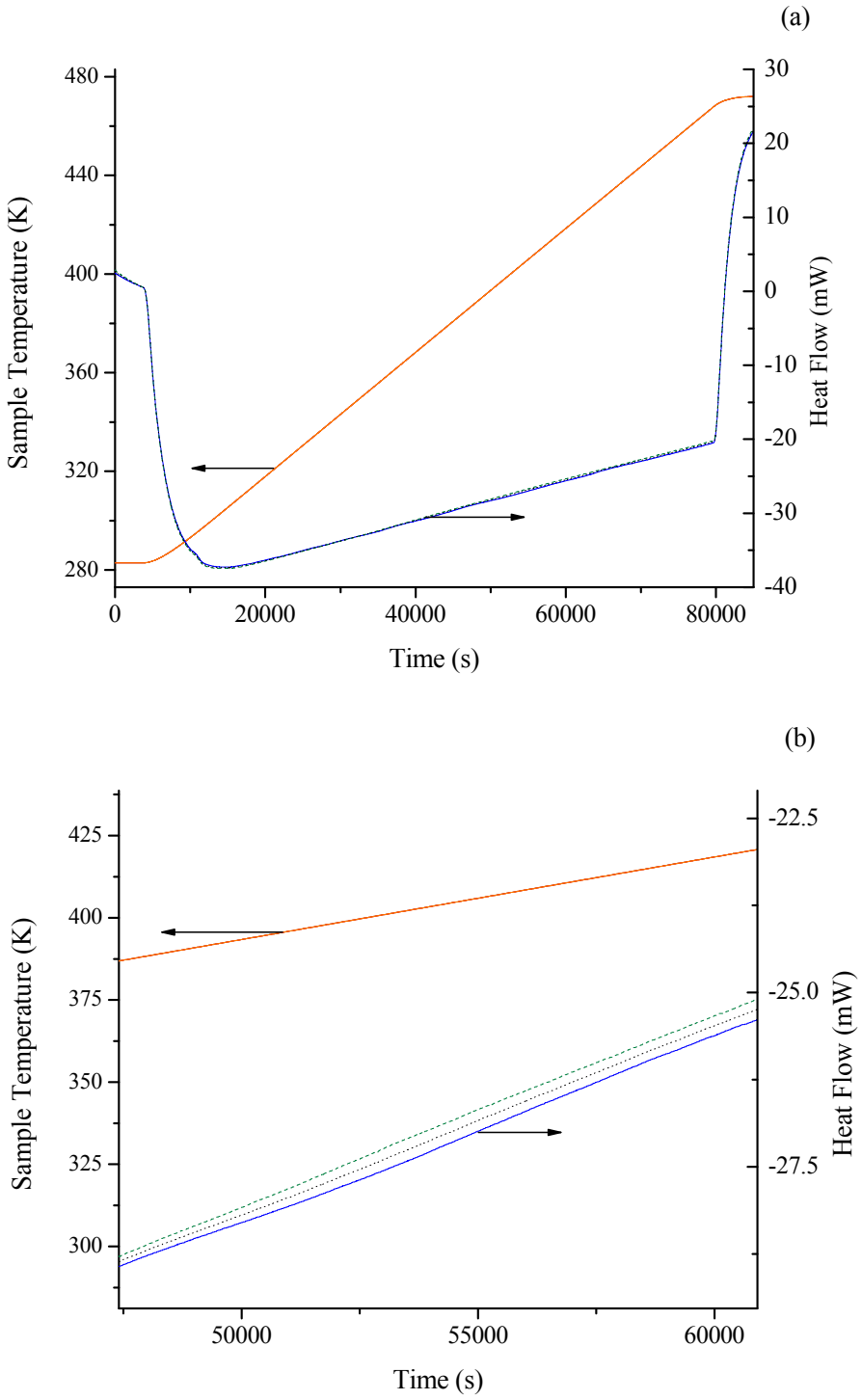

Figure 3. DSC curve for the blank tests performed using the continuous heating program at 4.0 MPa (solid line, blank test #1; dashed line, blank test #2; dotted line; blank test #3): (a), entire curve; and (b), zoom detail.

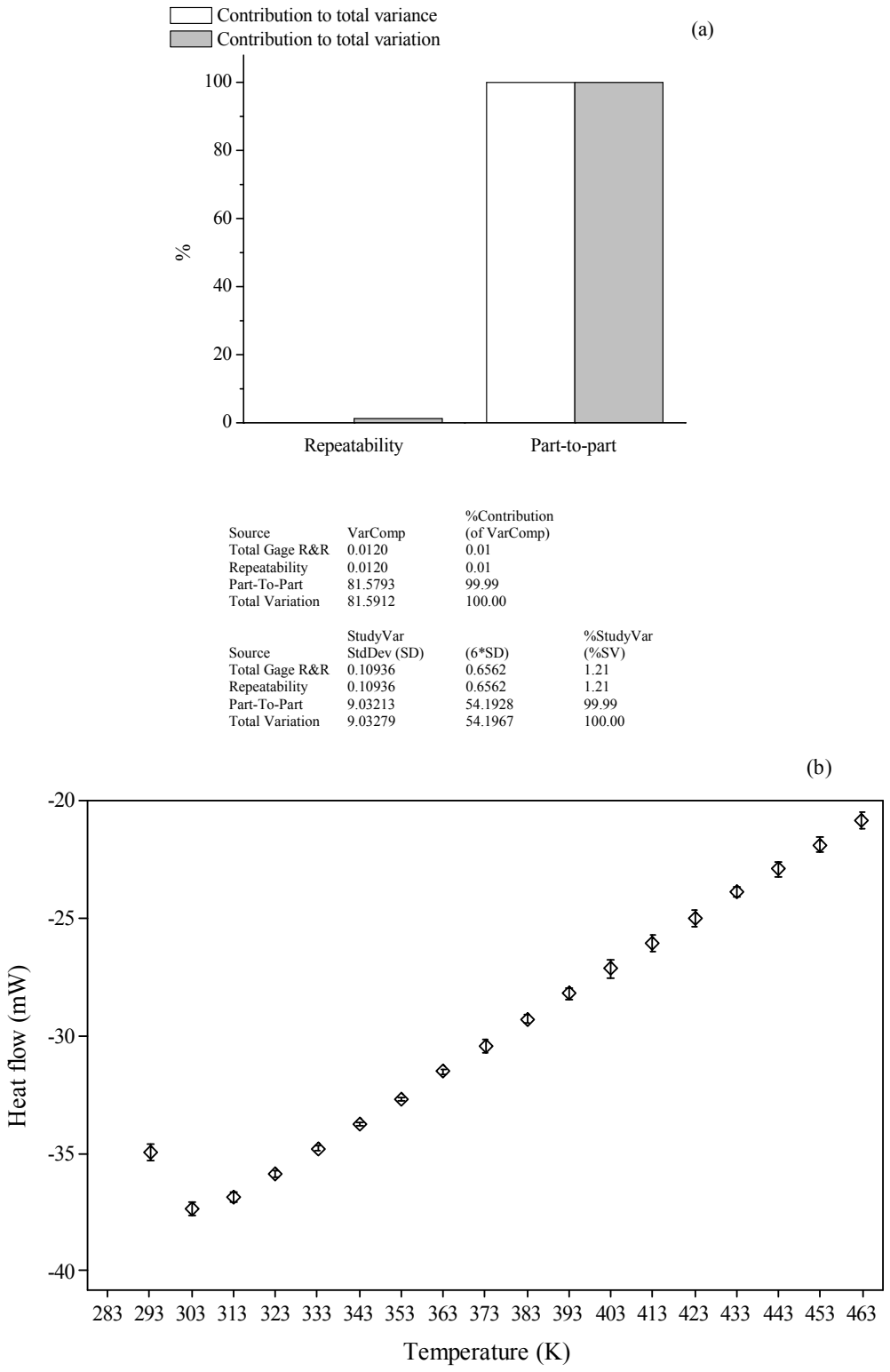

Figure 4. Results from the analysis of the measurement system variation: (a), Minitab output results from the crossed gage R&R study; and (b), interval plot for the means at 95% confidence level.

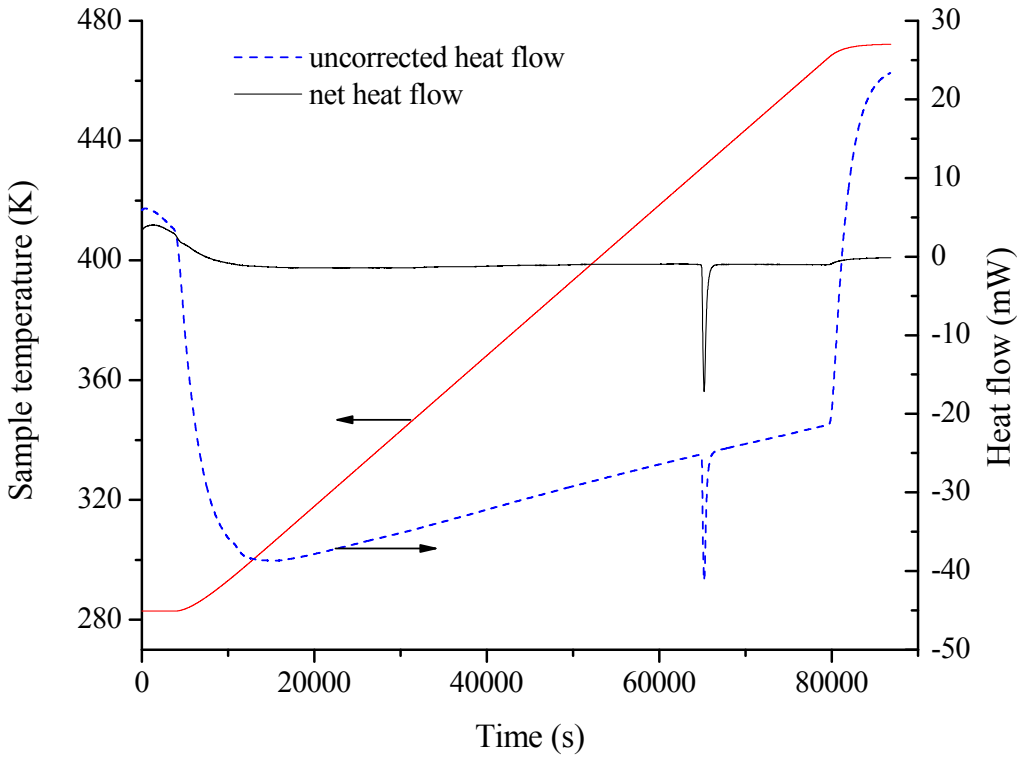

Figure 5. DSC curve for a representative indium test. The dashed line corresponds to the uncorrected heat flow signal, whereas the solid line corresponds to the net heat flow.

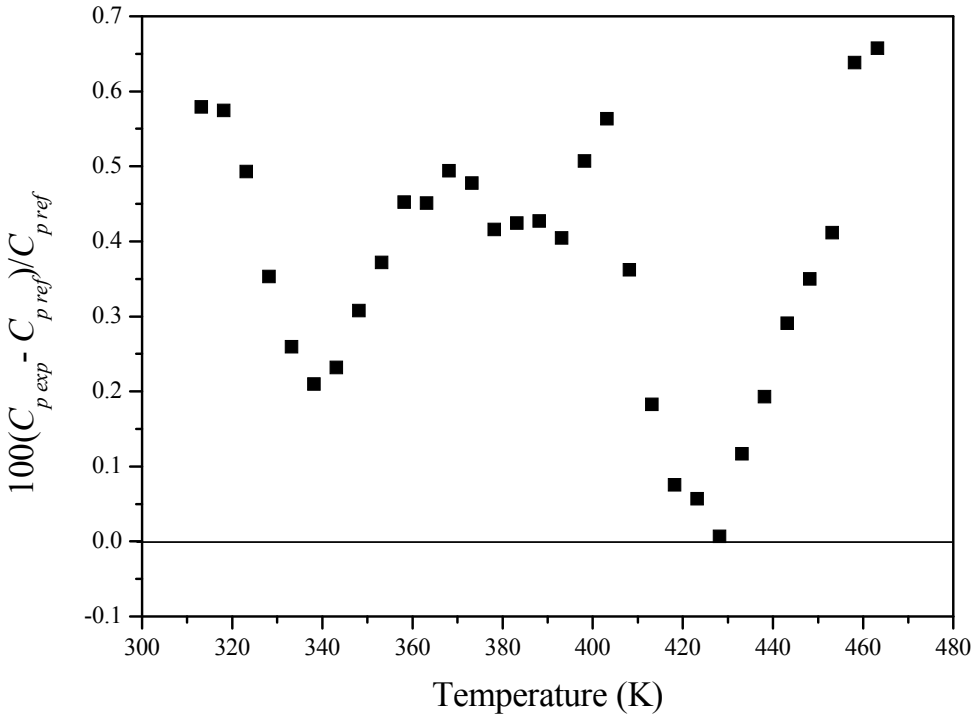

Figure 6. Differences, as a function of temperature, between experimental and reference values (NIST certificate) for specific heat capacity of synthetic sapphire at 0.1 MPa.

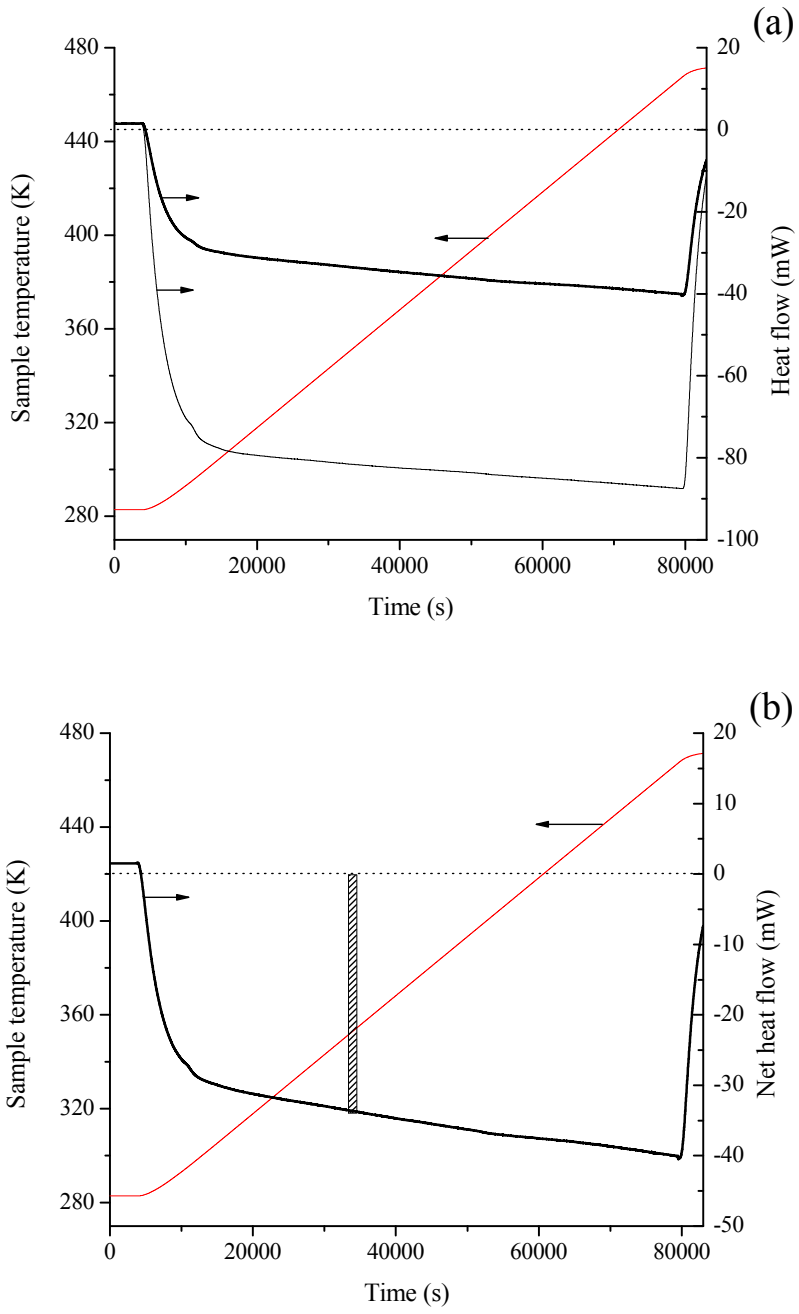

Figure 7. DSC curves for an experiment performed with sapphire at constant heating rate: (a), the thin solid line is the heat flow obtained for the blank test, and the bold solid line corresponds to the total heat flow; (b), the bold solid line is the net heat flow (which is obtained by subtracting the heat flow corresponding to the blank test from the total heat flow), the dotted line is the zero-constant baseline, and the shaded area is the integrated value of the net heat flow (assuming the zero-constant baseline) for a given average temperature (353.15 K).

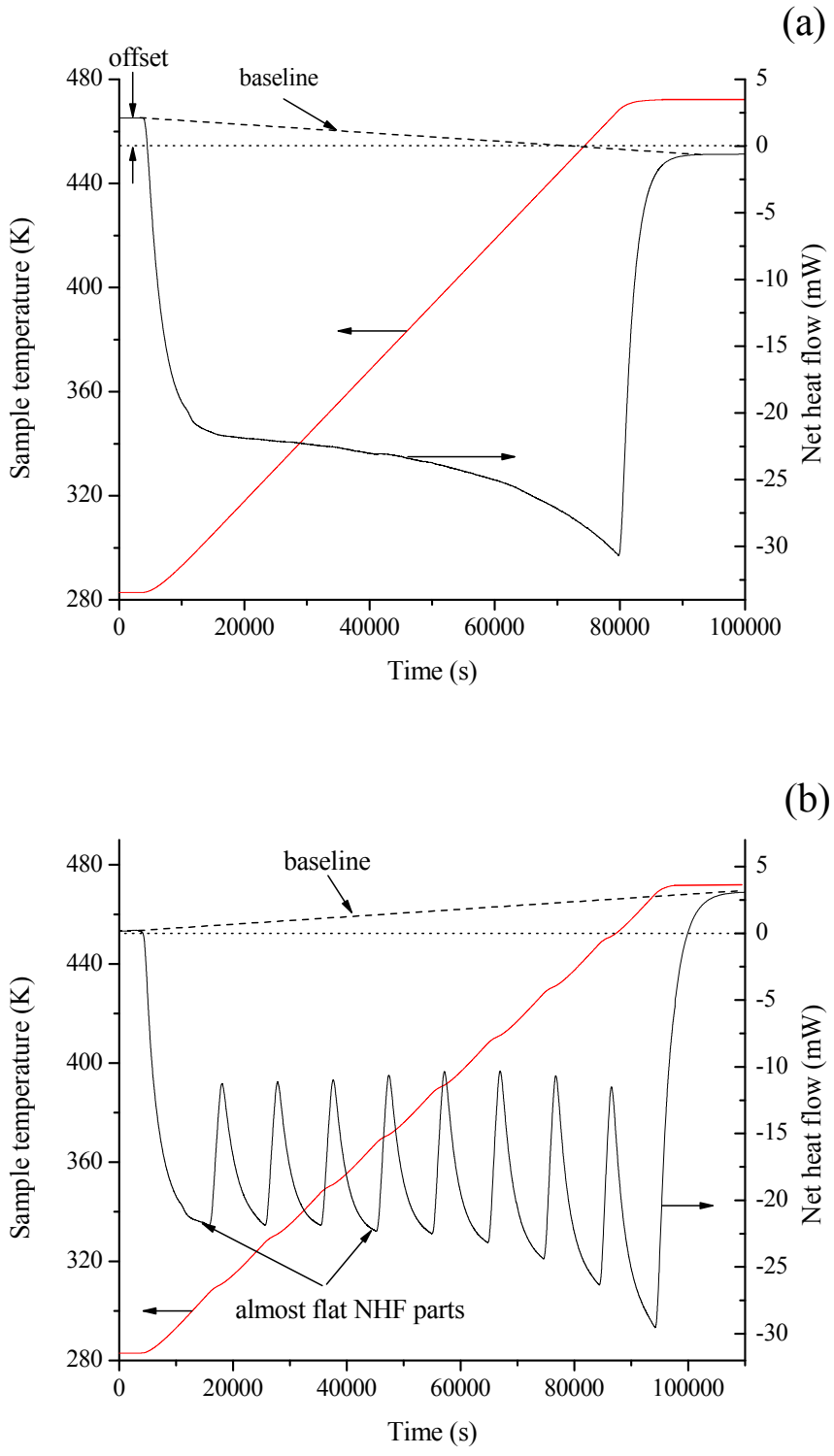

Figure 8. Examples of DSC curves obtained for pure water at a sample pressure of 4.0 MPa: (a), exp#7 using the continuous heating program (see Table 1); and (b), exp#10 using the stepwise heating program (see Table 1).

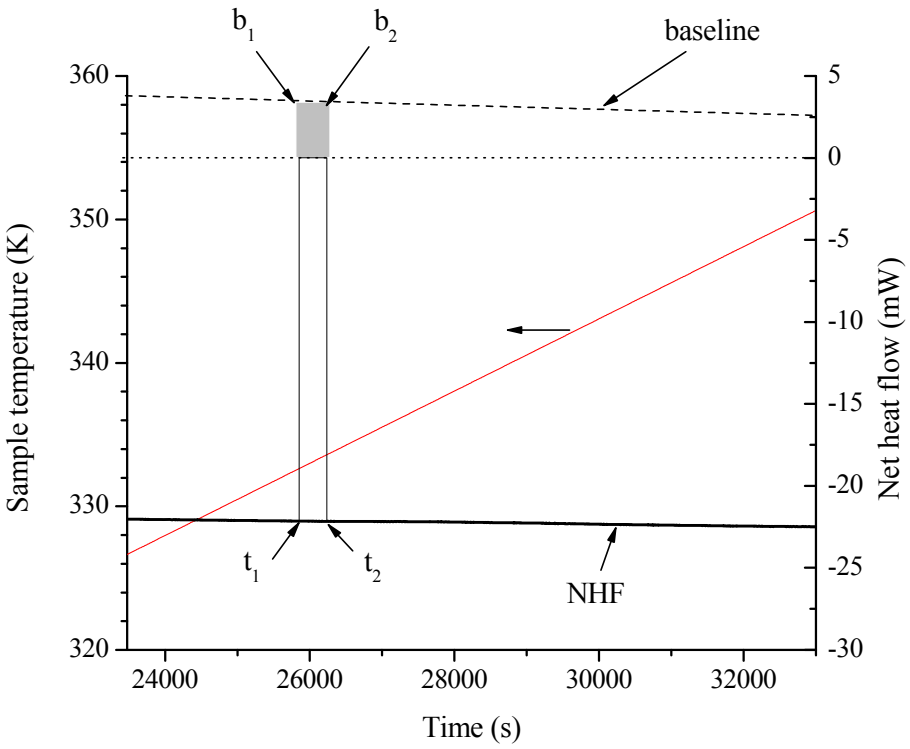

Figure 9. A graphical example of the procedure followed to determine the *I* values (exp#7 at a given average temperature of 333.15 K). The area of the gray trapezoid represents the second term of equation 5.

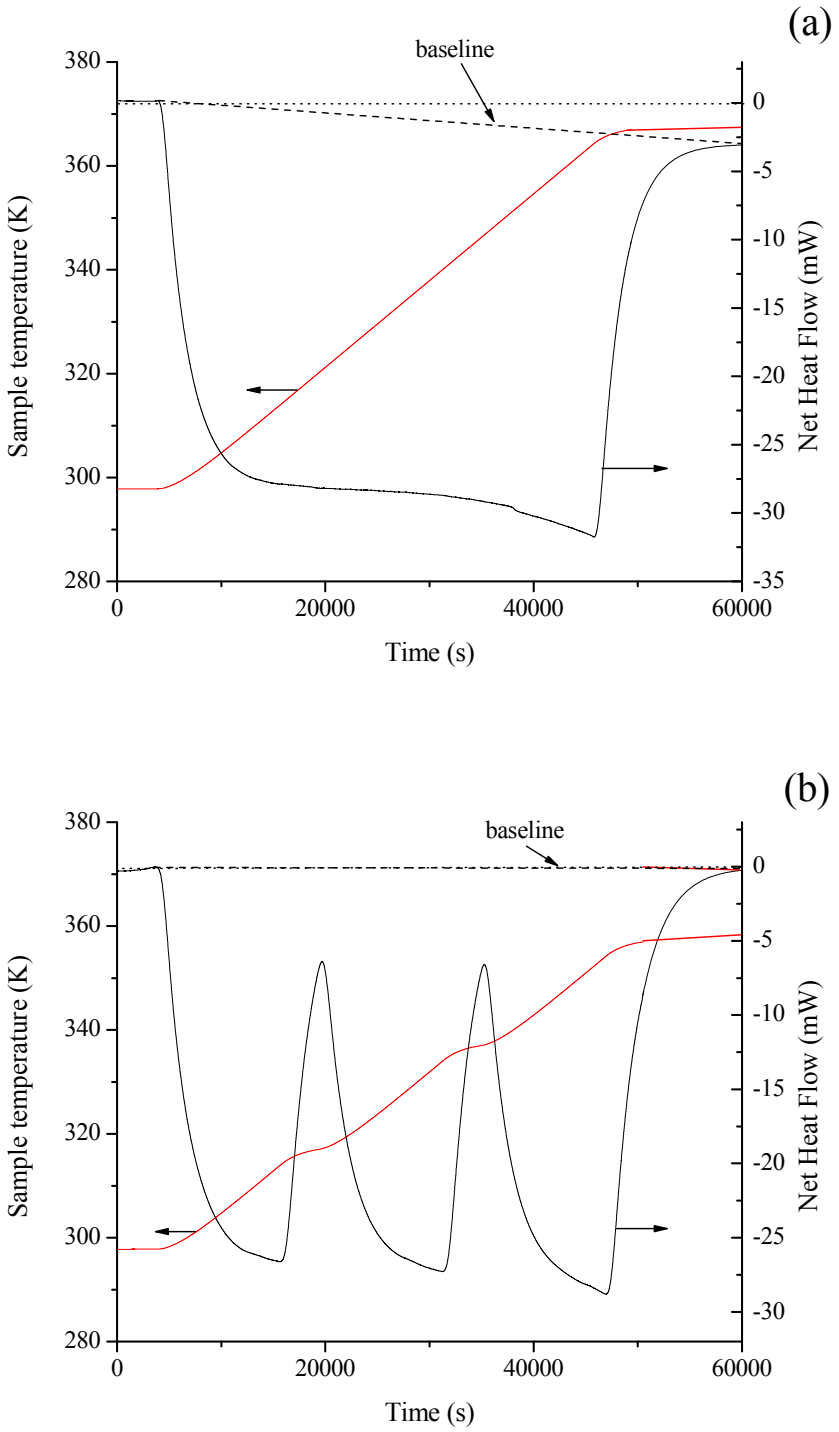

Figure 10. Examples of DSC curves obtained for pure water at a sample pressure of 0.1 MPa: (a), exp#1 using the continuous heating program (see Table 1) and (b), exp#4 using the stepwise heating program (see Table 1).

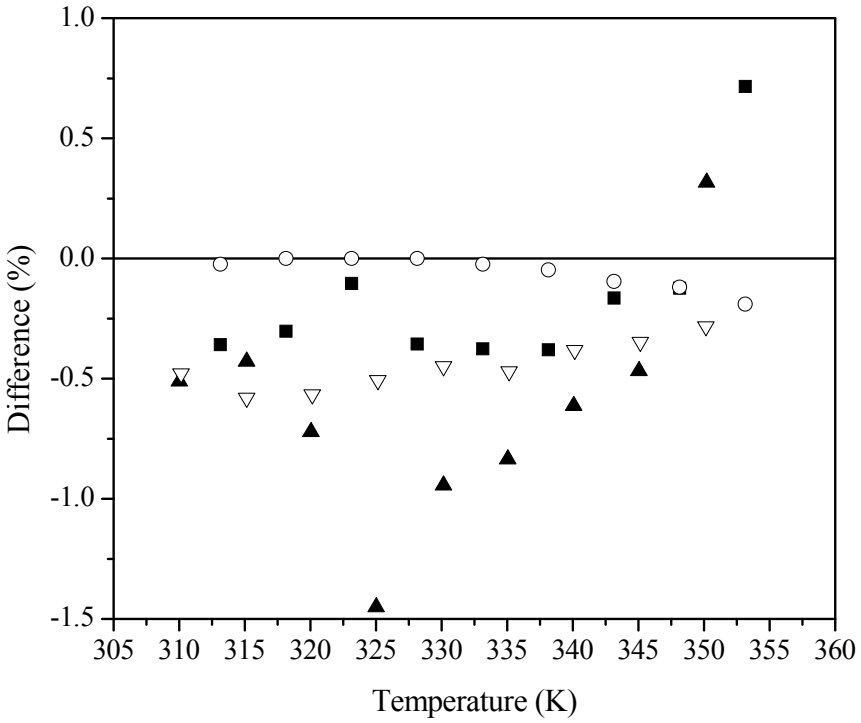

Figure 11. Differences, as a function of temperature, between measured (■, this study using the continuous heating program at 0.10 K min^{-1}; ▲, Lourenço and coworkers[23]; ▽, Diedrichs and Gmehling[27]; ○, Chiu and coworkers[41]) and reference values (IAPWS-95) for specific heat capacity of pure water at 0.1 MPa.

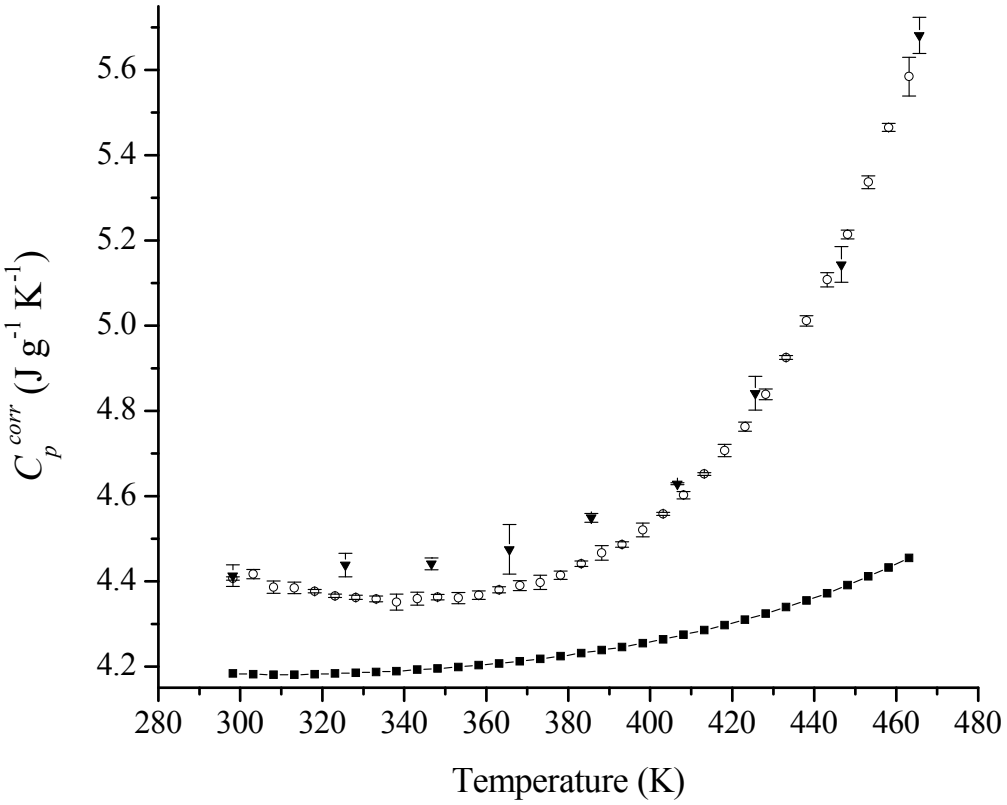

Figure 12. Comparison of C_p^{corr} values for pure water at 4.0 MPa (▼, this study using the stepwise heating method; ○, this study using the continuous heating method; ■, data from IAPWS-95).

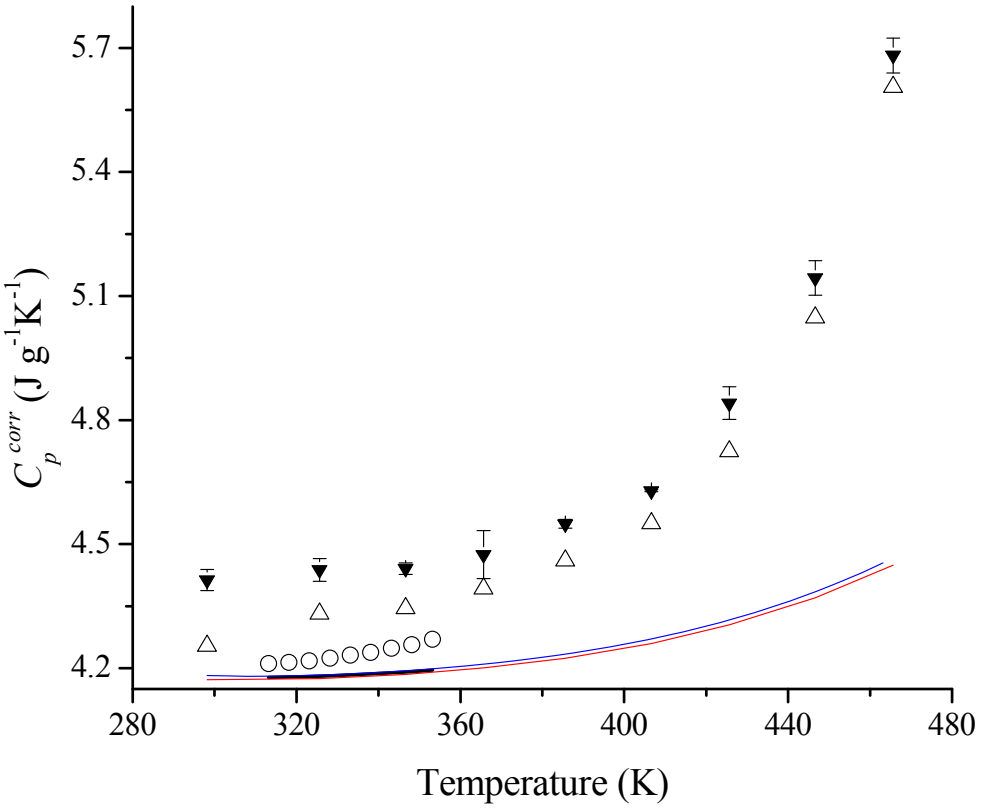

Figure 13. Differences between C_p^{corr} values obtained at different pressures (▼, at 4.0 MPa using the stepwise heating method; △, at 3.3 MPa using the stepwise heating method; ○, at 0.5 MPa from Setaram's lab using a C80 calorimeter under continuous heating rate conditions) and the corresponding reference values (black line, IAPWS-95 at 0.5 MPa; red line, IAPWS-95 at 3.3 MPa; blue line, IAPWS-95 at 4.0 MPa).

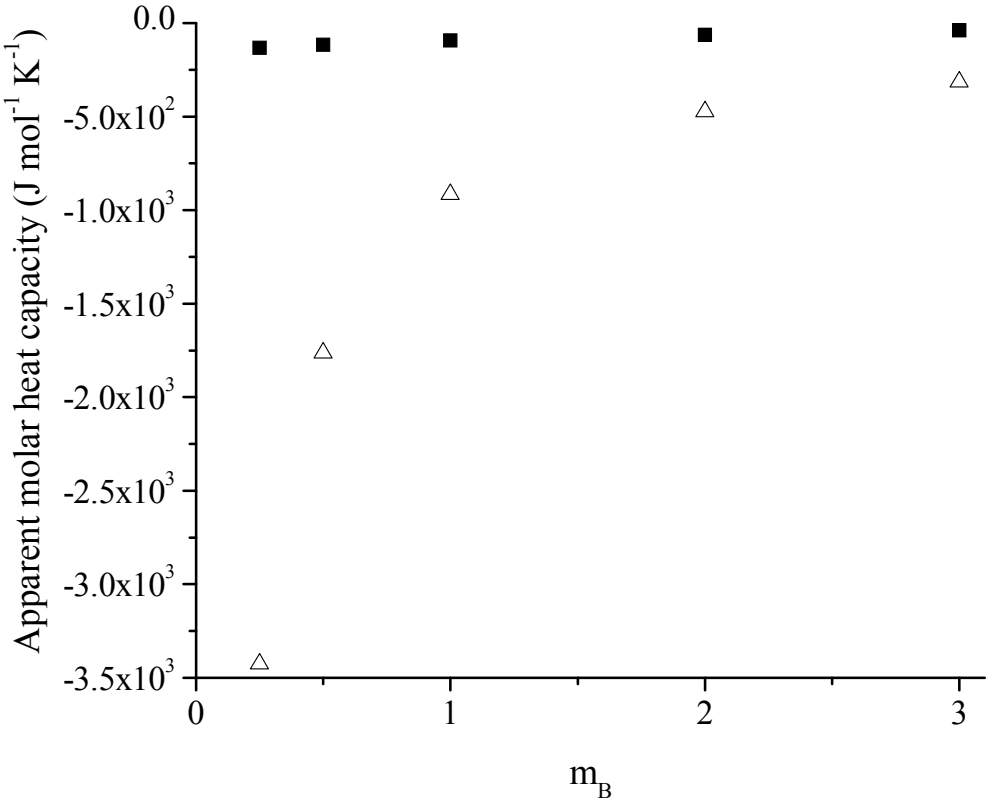

Figure 14. Apparent molar heat capacity of NaCl(aq) versus molality at 448.15 K and 4.0 MPa from measured $C_{p,s}$ data by Gates et al.[42] and: ■, the $C_{p,w}$ value assuming the IAPWS-95 formulation; △, the $C_{p,w}$ value reported in Table 5.